

**Dermal resident versus recruited $\gamma\delta$ T cell response to cutaneous
Vaccinia virus infection**

Amanda Swale Woodward Davis

A dissertation submitted in partial fulfillment
of the requirements for the degree of

Doctor of Philosophy

University of Washington

2014

Reading Committee:

Michael J. Bevan, Chair

Marion Pepper

Kevin B. Urdahl

Program Authorized to offer degree:

Department of Immunology

©2014
Amanda Swale Woodward Davis

Dedication

To all the science teachers, mentors, co-workers, classmates, friends and family who inspired, encouraged and supported me along the way – no one completes this journey on their own.

Table of Contents

Abstract.....	viii
List of Figures.....	ix
List of Tables.....	xi
Chapter 1: Introduction.....	1
The immune system: T cells.....	1
$\gamma\delta$ T cell development and function.....	2
The skin: resident T cell populations.....	4
Questions to address.....	5
Chapter 2: Materials and methods.....	6
Mice.....	6
Infections.....	6
Adoptive transfer of $\gamma\delta$ T cells and sorting.....	7
Adoptive transfer of OT-I T cells.....	7
Flow cytometry.....	8
Bone marrow chimeras.....	9
In situ proliferation.....	9
Cell transfer and in vivo proliferation.....	9
Cytokine analysis in the skin.....	10
Virus titration by plaque assay.....	10
Virus titration by qPCR.....	10
Histology.....	11
Immunofluorescence.....	11
Statistical analysis.....	12

Chapter 3: $\gamma\delta$ T cell functional subsets are determined during development, independent of TCR V γ chain use.....	13
Introduction.....	13
Results.....	14
<i>CCR6 and CD27 define distinct $\gamma\delta$ T cell subsets.....</i>	14
<i>A wave of $\gamma\delta$ T cells exit the perinatal thymus to form the circulating CCR6⁺CD27⁻ and dermal populations.....</i>	17
<i>Functional $\gamma\delta$ T cell subsets are determined independently of TCR Vγ chain expression.....</i>	19
Discussion.....	24
 Chapter 4: Vaccinia Virus infection results in accumulation of $\gamma\delta$ T cells in the tissue and alters the dermal $\gamma\delta$ T cell population.....	28
Introduction.....	28
Results.....	29
<i>$\gamma\delta$ T cells accumulate at the site of infection with the emergence of a novel dermal population</i>	29
<i>Circulating $\gamma\delta$ T cells are rapidly recruited to the VV infected ear.....</i>	31
<i>$\gamma\delta$ T cells show limited proliferation following infection.....</i>	35
<i>Adult BM- and pThy-derived $\gamma\delta$ T cells occupy discrete niches.....</i>	37
Discussion.....	40
 Chapter 5: Function and role of inflammatory resident and recruited $\gamma\delta$ T cells.....	44
Introduction.....	44
Results.....	45
<i>Loss of $\gamma\delta$ T cells does not impact inflammatory cytokine production in the tissue.....</i>	45
<i>$\gamma\delta$ T cells do not significantly impact the antigen specific CD8⁺ T cell response or resolution of infection.....</i>	45
<i>Inflammatory resident and recruited $\gamma\delta$ T cells are functionally distinct... </i>	48

<i>Resident dermal $\gamma\delta$ T cells enhance the early immune response to infection</i>	50
Discussion.....	52
Chapter 6: Concluding remarks and future directions.....	56
References.....	63

University of Washington

Abstract

Dermal resident versus recruited $\gamma\delta$ T cell response to cutaneous Vaccinia virus infection

Amanda Woodward Davis

Chair of the Supervisory Committee:
Professor and HHMI Investigator Michael J. Bevan
Department of Immunology

The study of T cell immunity at barrier surfaces has largely focused on T cells bearing the $\alpha\beta$ T cell receptor. However, T cells that express the $\gamma\delta$ T cell receptor are disproportionately represented in peripheral tissues of mice and humans, suggesting they too may play an important role responding to external stimuli. Here we report that in a murine model of cutaneous infection with Vaccinia Virus, dermal $\gamma\delta$ T cell numbers increased ten-fold in the infected ear and resulted in a novel $\gamma\delta$ T cell population not found in naïve skin. Circulating $\gamma\delta$ T cells were specifically recruited to the site of inflammation and differentially contributed to dermal populations based on their CD27 expression. Recruited $\gamma\delta$ T cells, the majority of which were CD27⁺, were Granzyme B⁺ and made up about half of the dermal population at the peak of the response. In contrast, recruited and resident $\gamma\delta$ T cell populations that made IL-17 were CD27⁻. Using a double chimera model that can discriminate between the resident dermal and recruited $\gamma\delta$ T cell populations, we demonstrated their divergent functions and contributions to early stages of tissue inflammation. Specifically, the loss of the perinatal thymus-derived resident dermal population resulted in decreased cellularity and collateral damage in the tissue during viral infection. These findings have important implications for our understanding of immune coordination at barrier surfaces and the contribution of innate-like lymphocytes on the front lines of immune defense.

List of Figures

Figure 3.1. Phenotype of $\gamma\delta$ T cells in the periphery of TCR δ -GFP mice.....	16
Figure 3.2. A wave of $\gamma\delta$ T cells exit the perinatal thymus (pThy) to form the circulating CCR6 ⁺ CD27 ⁻ subset and dermal $\gamma\delta$ T cells.....	18
Figure 3.3. $\gamma\delta$ T cell V γ expression in the circulation and skin.....	20
Figure 3.4. Functional $\gamma\delta$ T cell subsets are determined independently of TCR V γ chain expression.....	23
Figure 3.5. Model of $\gamma\delta$ T cell populations in the skin and skin dLN under steady state conditions.....	26
Figure 4.1. Following skin scarification with Vaccinia virus (VV), $\gamma\delta$ T cells accumulate in draining lymph node and dermis.....	30
Figure 4.2. Circulating $\gamma\delta$ T cells migrate to VV infected skin and contribute to all three dermal subsets.....	32
Figure 4.3. CD27 ⁺ $\gamma\delta$ T cells are only found in inflamed skin and contribute specifically to the CD103 ⁻ dermal population.....	34
Figure 4.4. Low level of $\gamma\delta$ T cell proliferation in situ following VV infection.....	36
Figure 4.5. Low level of transferred $\gamma\delta$ T cell proliferation and accumulation in vivo following VV infection.....	38
Figure 4.6. Contribution of adult BM-derived and perinatal thymus-derived $\gamma\delta$ T cells to the dermal response.....	39
Figure 5.1. Cytokine production in the ear following VV scarification.....	46
Figure 5.2. Loss of $\gamma\delta$ T cells does not impact antigen specific CD8 T cell response or viral load.....	47

Figure 5.3. Adult BM-derived and pThy-derived $\gamma\delta$ T cells in the dermis are functionally distinct..... 49

Figure 5.4. Absence of $\gamma\delta$ T cells reduces tissue pathology during VV infection..... 51

Figure 5.5. Dermal $\gamma\delta$ T cells accelerate early collateral damage and contribute to increased tissue cellularity during VV infection..... 53

Figure 6.1. Model of $\gamma\delta$ T cell response following scarification with VV..... 57

List of Tables

Table 3.1. $\gamma\delta$ T cell V γ genes, available antibodies and tissue localization.....	22
---	----

Chapter 1:

Introduction

The immune system: T cells

The immune system is a network of cells with diverse functions dedicated to identifying and eliminating pathogens. Within this network are the innate and adaptive immune systems, which respond to broad classes of pathogens and mount specific, long-lasting responses, respectively. Communication between the innate and adaptive systems is critical for successful removal of and long-term protection against infections. One half of the adaptive immune response are classical T cells, which express an $\alpha\beta$ T cell receptor (TCR) capable of recognizing foreign peptides in the context of self-MHC. The TCR dictates activation of T cells in the periphery and proper thymic selection ensures a TCR repertoire that is both diverse and non-reactive to host tissue.

More recently another lymphocyte subset was discovered that also develops in the thymus, but instead rearranges a TCR with γ and δ genes, termed $\gamma\delta$ T cells. Data suggests these cells receive a TCR signal in the thymus, although their TCR-responsiveness may be altered to play a less prominent role in their activation in the periphery (1, 2). It has been proposed that these cells instead are poised to implement effector functions rapidly in response to cytokines or innate stimuli through TLRs (3). As a result, $\gamma\delta$ T cells are considered part of the growing innate-like lymphocyte family, which also includes NK T cells and innate lymphoid cells. $\gamma\delta$ T cells have a mostly unknown TCR specificity, although a few ligands have been identified, none are recognized in a MHC-dependent manner (4).

$\gamma\delta$ T cell development and function

Although $\gamma\delta$ T cells are a minor population of lymphocytes in the circulation of mice and humans, they are enriched in peripheral tissues such as the gut and skin (5). This is in part due to their unique developmental programming, which results in waves of $\gamma\delta$ T cells being released from the thymus starting during fetal development of the mouse – a similar process also takes place during human fetal development (4). Each wave is characterized by transient and sequential expression of a single V γ chain and the earliest waves express an invariant TCR. Early in development $\gamma\delta$ T cells flood the circulation and seed peripheral tissues until soon after birth when $\alpha\beta$ T cells dominate and a small variety of $\gamma\delta$ T cells continue to be produced throughout life (4, 5).

Migration into peripheral tissues early in life is a hallmark characteristic of $\gamma\delta$ T cells. Previous studies have assessed the requirement for expression of various homing molecules, usually in the context of homeostasis and development (6). In the gut (CCR10 (7), CCR9 (8)) and skin (E/PSL, CCR4(9)), mice that lack expression have reduced $\gamma\delta$ T cells in their respective tissues. The first $\gamma\delta$ T cells to exit the thymus during embryonic development are dendritic epidermal T cells (DETC), which seed the murine epidermis and are not found elsewhere in the adult mouse (4). DETC express an invariant, germline encoded $\gamma\delta$ TCR (V γ 5/V δ 1). Although they are relatively immobile, their dendritic morphology allows them to sense keratinocyte health and plays a major role in the wound healing response (10-12). It has been proposed that their TCR recognizes a self ligand allowing them to rapidly respond to skin injury (13, 14). Similar clonal populations have also been found in the gut (V γ 7) and genital mucosa (V γ 6).

However, other tissues such as the lung and dermis are seeded in waves during development, but not with strictly clonal $\gamma\delta$ T cell populations.

A distinguishing characteristic of $\gamma\delta$ T cells is their ability to rapidly produce cytokines, which has also come to distinguish two major populations, IL-17- and IFN γ -producers. This functional commitment is thought to occur in the thymus and be controlled by TCR signal strength (1). On the whole, however, it is not clear what the TCR recognizes, either during development or in the periphery. Unlike $\alpha\beta$ T cells, $\gamma\delta$ T cells do not recognize antigen in a MHC-dependent manner and the structure of the TCR shares some similarities with the BCR. Some ligands for the $\gamma\delta$ TCR that have been identified in mice and/or humans are T10/T22, CD1c, MICA/B, phosphoantigens and the ATP synthase-1/apolipoprotein A-1 complex (15). The ability to recognize these structures does not appear to be constrained to a particular $\gamma\delta$ TCR, further complicating our understanding of their antigen specificity.

The existence of large clonal populations of $\gamma\delta$ T cells expressing identical or very similar TCRs calls into question their reliance on it for activation in the periphery. It is now appreciated that some $\gamma\delta$ T cells received a strong TCR signal in the thymus, making TCR stimulation virtually dispensable in the periphery (1). As a result, $\gamma\delta$ T cell functions may instead be controlled by innate sensors such as TLRs (16). Considering the DETC TCR is thought to recognize a self-ligand induced as a result of tissue damage, it is possible that many other $\gamma\delta$ T cell subsets perform a similar function. This also makes sense given the fact that their TCR repertoire is more limited and would not perform the same role as the antigen-specific $\alpha\beta$ T cell response.

The skin: resident T cell populations

The skin and its associated microbial flora are the body's first line of defense against infection. It is host to a network of immune cells that are in constant communication with commensal microbiota, keratinocytes and fibroblasts to maintain healthy tissue and respond quickly when the barrier is breached (17, 18). The initiation and requirements for residence of various immune subsets has been of great interest. T lymphocytes are one such cell type capable of permanent residence within the tissue, although some are more short lived (17, 18). Following antigen-specific activation in central lymphoid organs, TCR $\alpha\beta$ effector cells traffic to peripheral sites, including the skin, and some become resident memory T cells (T_{RM}). These cells are recruited into the tissue as a result of local infection or inflammatory signals and remain there to protect against future external insults (19-24).

Two populations of $\gamma\delta$ T cells are found in the skin. DETC, which have been mentioned above, are a relatively immobile population in the epidermis. They function to maintain keratinocyte health, sense tissue damage and aid in the repair process. More recently discovered are dermal $\gamma\delta$ T cells. In contrast to TCR $\alpha\beta$ T_{RM} cells, TCR $\gamma\delta$ T cells have been shown to home to the dermis and acquire specific functions as a result of developmental programming and their response via TCR recognition of foreign antigens in poorly defined (25-27). We and others have observed that dermal $\gamma\delta$ T cells appear to be a more motile and diverse population and comprise up to half of the dermal T cells in mice (28) and 2-9% in humans (29).

This population has been shown to participate in host defense against bacterial infection of the skin (28, 30) as well as to contribute to psoriasis in the mouse (31, 32)

and humans (33). It is now appreciated that in mice, dermal $\gamma\delta$ T cells exit the thymus and seed the dermis near the time of birth (27, 34). Characterization of dermal $\gamma\delta$ T cells by several groups has revealed their memory phenotype and functions related to that of $CD4^+$ T_H17 cells, being capable of producing IL-17 upon stimulation *in vitro*. Dermal $\gamma\delta$ T cells express CCR6, CXCR6, CD103, CD44, IL-23R and IL-7R (33-35). However, it is unclear whether IL-17-producing dermal $\gamma\delta$ T cell populations observed during infection or inflammation are derived from the resident population seeded there at birth or if unique populations are recruited from the circulation.

Questions to address

Given the mysterious nature of $\gamma\delta$ T cells and their unconventional attributes, it is not surprising that we still have a great deal to learn about how they function within the immune system. Here we use a system of localized infection to investigate migration, plasticity and function of $\gamma\delta$ T cells and put these within the context of development. The importance of immune coordination at barrier surfaces is being increasingly recognized for its ability to offer protection (21) or in some cases cause harm to the organism (36). The primary characteristics that we understand about $\gamma\delta$ T cells are their unique programming to reside in barrier tissues and respond rapidly to inflammatory stimuli, which lends them well to helping maintain immunity to pathogens. Therefore, elucidating how $\gamma\delta$ T cells participate in the immune response at these sites is imperative for a complete understanding of barrier immunity.

Chapter 2:

Materials and methods

Mice

C57BL/6, B6.SJL-Ptprc^a Pepc^b/BoyJ and TCR $\delta^{-/-}$ mice were obtained from the Jackson Laboratory and TCR δ -H2BeGFP (TCR δ -GFP) mice were obtained from I. Prinz (Hannover Medical School) and have been described previously (37). Mice were housed in specific pathogen-free conditions in the animal facilities at the University of Washington and unless otherwise specified were used at 6-10 weeks of age. All experiments were done in accordance with the Institutional Animal Care and Use Committee guidelines of the University of Washington.

Infections

2×10^6 plaque forming units (PFU) of recombinant Vaccinia Virus expressing full-length chicken ovalbumin (VV-OVA) was used for epicutaneous infection by skin scarification, as described previously (37). Mice were anesthetized with isoflurane and 5 μ l of diluted virus was applied to the dorsal side of the ear. The skin area was then gently scratched 20 times with a 28-gauge needle. For flow cytometry experiments, both ears of mice were infected and combined to comprise one sample and the numbers were divided by two to obtain the number of cells/ear. VV-GFP was used for immunofluorescence experiments.

Adoptive transfer of $\gamma\delta$ T cells and sorting

C57BL/6 or CD45.2⁺ TCR δ -GFP mice received 7×10^5 $\gamma\delta$ T cells enriched from spleen and skin dLN of CD45.1⁺ TCR δ -GFP mice by i.v. injection one day before infection. Enrichment of $\gamma\delta$ T cells was performed by incubating single cell suspensions with biotin-labeled anti-TCR β and anti-CD19 mAb for 30 minutes on ice, followed by passage through the Stem Cell Biotin negative selection kit. Mice were infected on one ear and the infected (or uninfected) ears from two mice were combined for each sample. In some experiments, the enriched population was further purified as follows: cells were stained with fluorochrome-conjugated anti-CD27 and sorted on a FACS Aria for the GFP⁺TCR β ⁻CD19⁻CD27⁺ or GFP⁺TCR β ⁻CD19⁻CD27⁻ populations, of which >97% were TCR $\gamma\delta$ ⁺. 6×10^5 CD27⁺ or 2.7×10^5 CD27⁻ sorted $\gamma\delta$ T cells from B6.SJL-Ptprc^a Pepc^b/BoyJ (CD45.1) mice were transferred into separate C57BL/6 (CD45.2) hosts. Mice that received sorted cells were infected on both ears and ears from a single mouse were combined for a sample.

Adoptive transfer of OT-I T cells

Spleen and LN from GFP OT-I mice (whose CD8 T cells recognize the SIINFEKL peptide in OVA) were harvested and single cell suspensions obtained. The BD Biosciences CD8 T cell enrichment kit (plus CD44-Biotin) was used to enrich for OT-I T cells. Purity was determined and 1×10^4 OT-I s were transferred into each mouse.

Flow cytometry

Single cell suspensions were prepared from spleens and LN by mechanical disruption. Dorsal and ventral halves of ears were separated, minced and then enzymatically digested for 2 hrs at 37 °C in Liberase TM (Roche). Both ears from each mouse were combined for processing to obtain adequate cell numbers. All tissues were passaged through a 100- μ m nylon sieve (BD Bioscience). In some experiments, to avoid the Liberase digestion (which cleaved CD27), dorsal and ventral halves of the ears were separated and floated dermal side down in complete media overnight at 37°C. Supernatant, into which cells had migrated, was collected the following day and stained. Cells were stained for 30 min on ice with the appropriate mixture of monoclonal antibodies and washed with PBS containing 1% BSA. The following conjugated mAb were obtained from BD Pharmingen, eBioscience or BioLegend: anti- TCR β (H57-597), CCR6 (140706), CD27 (LG.3A10), CD103 (2E7), V γ 5 (BioLegend V γ 3 clone 536), CD44 (IM7), CD45.1 (A20), CD45.2 (104). In the ear, $\gamma\delta$ T cells from TCR δ -GFP were identified as GFP⁺V γ 5⁻ (dermal) or GFP⁺V γ 5⁺ (DETC), according to the nomenclature described by Heilig & Tonegawa (38). For the analysis of intracellular IFN γ , IL-17 and Granzyme B, single cell suspensions were incubated in the presence or absence of 50 ng/mL PMA and 500 ng/mL Ionomycin for 4 hours at 37°C in the presence of Brefeldin A. Cells were stained for surface markers and then processed using the BD PharMingen Cytofix/Cytoperm kit. For analysis of Ki67, cells were stained for surface markers and then processed using the eBioscience FoxP3 kit. Samples were analyzed on a FACSCanto II (BD) using Flowjo software (Tree Star).

Bone marrow chimeras

Chimeras were made as previously described (22). Briefly, perinatal thymocytes (pThy) were harvested 0–48 h after birth and 5×10^6 cells were transferred i.v. to congenic recipients that had been lethally irradiated with a dose of 1000 rad in a cesium irradiator. The next day, $1-2 \times 10^6$ congenic bone marrow (BM) cells were transferred. These mice are referred to as “BMpThy chimeras” while controls without pThy are referred to as “BM chimeras”. Chimeras were analyzed or infected at least 8 weeks after reconstitution.

In situ proliferation

Infected mice were injected i.p. with 2mg in 200 μ l 50-Bromo-2-deoxyuridine (BrdU) 1 hour before being euthanized. Single cell suspensions were obtained from each tissue and stained using the BD Biosciences APC BrdU Kit. Cells were fixed with PFA before Cytotfix/Cytoperm to ensure retention of TCR δ -GFP signal.

Cell transfer and in vivo proliferation

Cells were harvested as described for cell transfer experiments and labeled for 20 minutes at room temperature with 5 μ M of CellTrace Violet (CTV, Life Technologies). Following incubation cells were washed in serum, resuspended in PBS and $6-7 \times 10^6$ $\gamma\delta$ T cells were transferred into each mouse. For analysis of CTV dilution cells only live cells were gated on.

Cytokine analysis in the skin

Ears from infected mice were harvested, split open and added to tubes with 1 mL of cytokine extraction buffer (1 mini protease inhibitor/10mL, 0.4M NaCl, 0.5% BSA, 10mM EDTA, 0.05% Tween, 0.1mM benzethonium chloride) and beads. Tubes were placed in a bead beater for two 90 sec intervals (placed on ice in between). After homogenization, tubes were incubated on ice for 10 minute before being centrifuged for 5 min at 1300rpm. 500µl of the supernatant was transferred to a spin-x filter tube and centrifuged for another 5 min. Flow through was frozen at -80°C and thawed only once before use. For analysis of cytokines, the protocol for the BD Biosciences Cytometric Bead Array (CBA) Inflammation Kit was followed. Amount of each cytokine in the tissue was determined with standards provided in the kit and calculated based on MFI.

Virus titration by plaque assay

The viral load in organs was determined by plaque assays on 143B cells with dilutions of a 40% tissue homogenate added to confluent wells. Organs were harvested and homogenized in PBS using a bead beater. Samples were kept at -80°C and were frozen and thawed 3 times before being used. Titers reported are log₁₀ PFU per whole LN or ear.

Virus titration by qPCR

Tissue samples were harvested and DNA was purified with the DNeasy Mini Kit (Qiagen 69504). The primers used in the quantitative PCR assay are specific for the ribonucleotide reductase Vv14L of VV. The sequences are: (Fwd)

TTGTAGAATACCGTTACTGGCG and (Rev) CTTGTGCTTCCAGGCTATCA. Control primers from GAPDH are: (Fwd) CAATGGCTTGTTCCTACTGCC and (Rev) CCAACAGGACCTCAGCCC. Amplification reactions were performed in a 96-well PCR plate (Bio-Rad Laboratory) in a 25µl volume containing 2x SybrGreen Master Mix (Applied Biosystems), 0.5µM forward primer, 0.5µM reverse primer and the template DNA. Thermal cycling conditions were: 95° C for 10 min, 94°C for 15 sec and 63°C for 1 min (45X). To calculate the virus load, a standard curve was established from DNA of a VV stock with previously determined titer. Corresponding CT values obtained by the real-time PCR methods were plotted on the standard curve to estimate viral load in the skin samples.

Histology

Ears from infected mice were fixed in 10% buffered formalin for 3 days before being embedded vertically in paraffin. Sections were hematoxylin and eosin stained and the severity of inflammation and necrosis was determined on a scale of 0-4 (4 being the most severe). Scoring of all samples was blinded and uninfected mice were used as controls.

Immunofluorescence

Epidermal peels were obtained by a method given to us by the Havran Lab (11). Briefly, dorsal and ventral sides of the ears were separated and floated in a petri dish in a solution of 3.6% ammonium thiocyanate for about 15 min at 37°C. Epidermis could then be gently removed and transferred to a new dish to be stained. For skin cross-sections,

back skin was treated with Nair to remove hair and a small section cut and rolled before being frozen in Optimal Cutting Temperature (OCT) medium. Sections were cut, dried overnight and fixed in acetone before being stained. The following antibodies were used: $\gamma\delta$ TCR-PE, V γ 5-APC, CD3-PE.

Statistical analysis

Prism software (GraphPad) was used for all statistical analysis. The two-tailed, unpaired student *t*-test was used for comparisons of $\gamma\delta$ T cell frequencies and histological scores.

Chapter 3:

$\gamma\delta$ T cell functional subsets are determined during development,
independent of TCR V γ chain use

Introduction

$\gamma\delta$ T cells were discovered over 30 years ago and originally noted for their prevalence during fetal development (38). Subsequent studies determined that $\gamma\delta$ T cells exit the thymus in waves, which correlate with the use of specific TCR V γ chain usage and homing to different tissues (5). Although few $\gamma\delta$ T cells are found in the adult circulation, they are greatly enriched in peripheral tissues (5, 39). Considering $\gamma\delta$ T cells were discovered because of their unique use of V γ and V δ genes, they have long been defined and subsetted based on their TCR expression. However, recent data suggests that the TCR may be dispensable for activation of some $\gamma\delta$ T cells in the periphery (1, 40, 41) and other cell surface markers might be more accurate for describing lineages within the population.

It has been proposed for some time that $\gamma\delta$ T cell function is determined in the thymus (2, 25, 42). Emerging data from studies of $\gamma\delta$ T cells in central lymphoid organs suggest that CD27 delineates $\gamma\delta$ T cell functional subsets (27, 41, 43). On activated $\alpha\beta$ T cells, CD27 is thought to enhance survival and proliferation via interaction with CD70 (44). However, CD27 expression on $\gamma\delta$ T cells appears to identify subsets determined during development and its expression by mouse $\gamma\delta$ T cells is tightly correlated with their ability to produce IFN γ , whereas failure to express CD27 correlates with IL-17 production (43). Importantly, analogous $\gamma\delta$ T cell populations have been found in human

PBMC (45-47), making this a relevant axis from which to orient experiments in model organisms.

Although these populations have been described in the circulation, their relevance to $\gamma\delta$ T cell populations in peripheral tissues such as the skin has not been investigated. Several cell surface proteins have been used to characterize dermal $\gamma\delta$ T cells, in particular CD103 and CCR6 are readily found on this population. A recent study identified a population of $\gamma\delta$ T cells enriched in the skin dLN of mice that share similar properties with dermal $\gamma\delta$ T cells (34). This discovery demonstrated a potential link between dermal $\gamma\delta$ T cells and those found in the circulation. We used a combination of these markers in an attempt to relate known lineages to functional subsets associated with the tissue and determine how this might tie into developmental programming.

Results

CCR6 and CD27 define distinct $\gamma\delta$ T cell subsets

The only unique marker to $\gamma\delta$ T cells is their TCR. Staining for the $\gamma\delta$ TCR is not always clear or possible as some $\gamma\delta$ T cells down-regulate the TCR upon activation. Further, for *in vitro* or transfer experiments it is not ideal to have an antibody attached to the TCR. In order to cleanly identify $\gamma\delta$ T cells and use them untouched in some experiments, we obtained mice which express GFP under the TCR δ promoter (37). Mice are bred homozygous without impacting TCR expression, ensuring that all $\gamma\delta$ T cells are GFP⁺. GFP is bound to histones in the nucleus making intracellular staining possible without the loss of fluorescence. One caveat is that a small fraction of $\alpha\beta$ T cells express GFP as a result of attempts to rearrange a productive TCR in the thymus;

this residual GFP is most likely on $\alpha\beta$ T cells that have recently emigrated (48). In the circulation $\alpha\beta$ T cells make up approximately half of the GFP⁺ cells, but almost none are found in the skin. A GFP^{lo} population can also be found and these have been described as NK cells (49). Therefore we identify $\gamma\delta$ T cells as TCR β ⁻GFP⁺ in all our experiments (Figure 3.1A).

Staining of $\gamma\delta$ T cells in the skin dLN revealed that CD27 and CCR6 were mutually exclusive in peripheral lymphoid organs and identified three $\gamma\delta$ T cell populations (Figure 3.1A) with distinct surface and transcription factor staining patterns (Figure 3.1B). In line with previous reports that CD27⁻ $\gamma\delta$ T cells produce IL-17 upon stimulation, we found that baseline expression of the transcription factor ROR γ t was higher in CD27⁻ than in CD27⁺ $\gamma\delta$ T cells. Conversely, the transcription factor Tbet was highest in the CD27⁺ $\gamma\delta$ T cells. CCR6⁺CD27⁻ $\gamma\delta$ T cells expressed the highest levels of CD44 and CD103, while the small number of CD27⁻CCR6⁻ cells and the CD27⁺ cell subset had lower levels of CD44 and only half expressed CD103. Upon stimulation of naïve $\gamma\delta$ T cells from the skin dLN with PMA/Ionomycin for 4 hours, IFN γ was produced by CD27⁺ $\gamma\delta$ T cells and IL-17 was produced by CD27⁻CCR6⁺ $\gamma\delta$ T cells (Figure 3.1C). Despite their phenotypic similarity, the CD27⁻CCR6⁻ $\gamma\delta$ T cells produced little of either cytokine suggesting this population may have different functions and/or requirements for cytokine production.

Although there is significant evidence to suggest CD27 expression marks separate populations, it has not been definitively proven that they are independently maintained. Further, since there is lack of clarity on the subject, previous studies have interpreted changes in the CD27 ratio to be due to up- or down-regulation of this marker

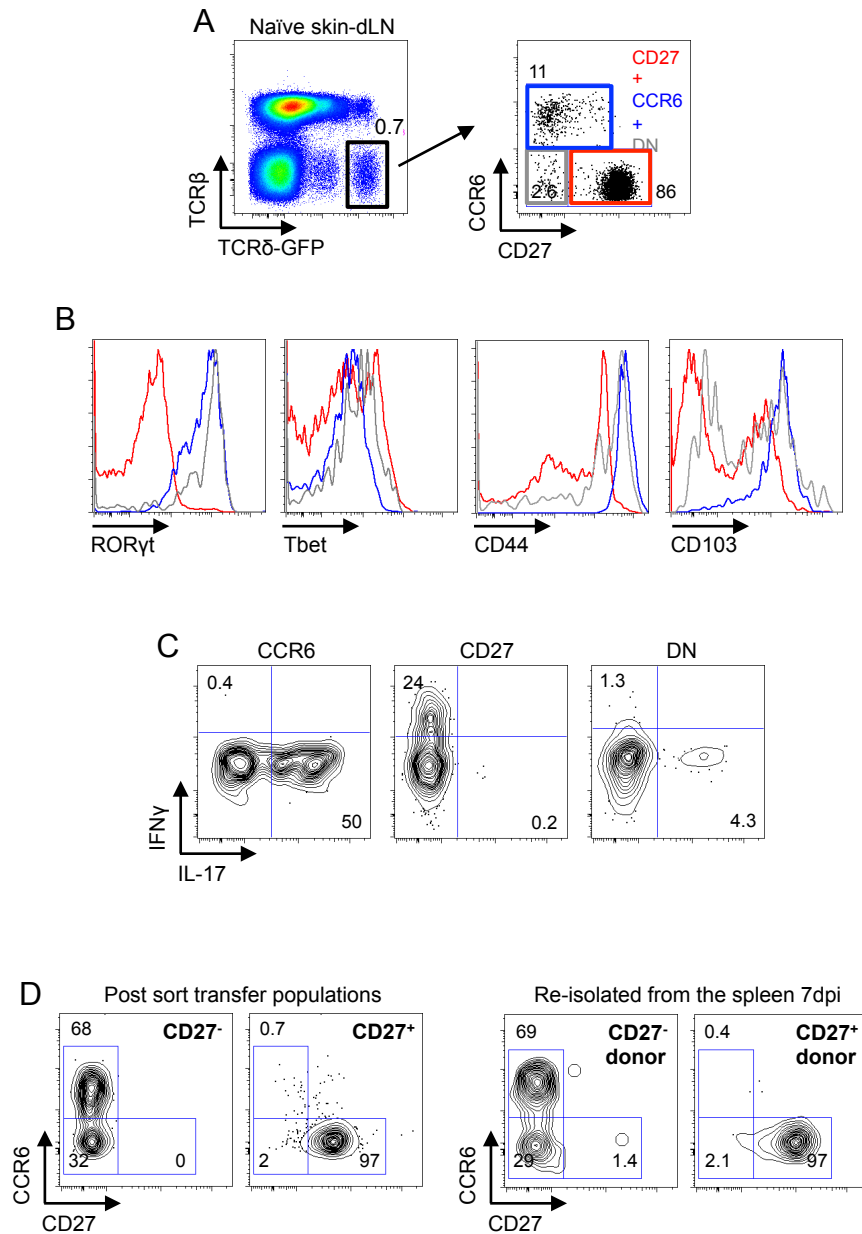


Figure 3.1. Phenotype of $\gamma\delta$ T cells in the periphery of TCR δ -GFP mice. A) Representative flow plots show gating strategy for $\gamma\delta$ T cells in the skin dLN and CCR6 by CD27 profile. Numbers denote percent of total dermal $\gamma\delta$ T cell population within the indicated quadrant. B) Nuclear and surface staining for ROR γ t, Tbet, CD44 and CD103 on the three circulating $\gamma\delta$ T cell populations. Colored boxes in A correspond with histograms. C) Single cell suspension from the skin dLN of naïve mice was re-stimulated with PMA/Ionomycin for 4 hours at 37°C followed by intracellular staining for cytokines. Representative flow plots are shown and gates are based on unstimulated naïve samples. Numbers indicate the percentage of that population in each quadrant. D) $\gamma\delta$ T cells from spleen and skin dLN of TCR δ -GFP mice were sorted based on CD27 expression and 6×10^5 CD27⁺ or 2.7×10^5 CD27⁻ $\gamma\delta$ T cells were transferred into separate C57BL/6 hosts. Recipients were infected with VV on the ear the following day. Flow plots show the phenotype of CD27⁻ and CD27⁺ at the time of transfer and 7dpi in the spleen. Numbers denote the percentage of cells within the indicated quadrant.

rather than expansion of one population. To ask whether CD27 is indeed a stable marker of $\gamma\delta$ T cell lineages in the presence of inflammation, CD27⁺ and CD27⁻ $\gamma\delta$ T cells were sorted from mice and transferred into separate congenically marked hosts. On day 7 post infection transferred cells were re-isolated from the spleen and stained for CD27 as well as CCR6. At this time point, no cells from either group changed their expression of CD27 (Figure 3.1D). It is also interesting to note that the ratio of CCR6⁺ and CCR6⁻ $\gamma\delta$ T cells within the CD27⁻ subset was relatively unchanged. These experiments demonstrate that in vivo in the presence of inflammatory signals, CD27 expression in the circulation remains constant as a marker of distinct $\gamma\delta$ T cell lineages.

A wave of $\gamma\delta$ T cells exit the perinatal thymus to form the circulating CCR6⁺CD27⁻ and dermal populations

Previous studies have demonstrated that near the time of birth, $\gamma\delta$ T cells exiting the thymus contribute to the circulating CD27⁻ population (27) and dermal $\gamma\delta$ T cells (34). We analyzed the adult and perinatal (0-48 hours after birth) thymus to determine whether mature $\gamma\delta$ T cell thymocytes (GFP⁺TCR $\gamma\delta$ ⁺) differed in CCR6 and CD27 expression. In the adult thymus $\gamma\delta$ T cell subsets reflected closely the phenotype of the circulating population. In contrast, a much higher proportion of perinatal $\gamma\delta$ T cells are CD27⁻, and more specifically express CCR6 (Figure 3.2A).

A model was recently described to validate the existence of this wave and its unique ability to contribute to the dermal $\gamma\delta$ T cell population (34). Following lethal irradiation, we confirmed that $\gamma\delta$ T cells in the circulation and dermis are sensitive to whole body irradiation. Although donor bone marrow (BM)-derived $\gamma\delta$ T cells were the

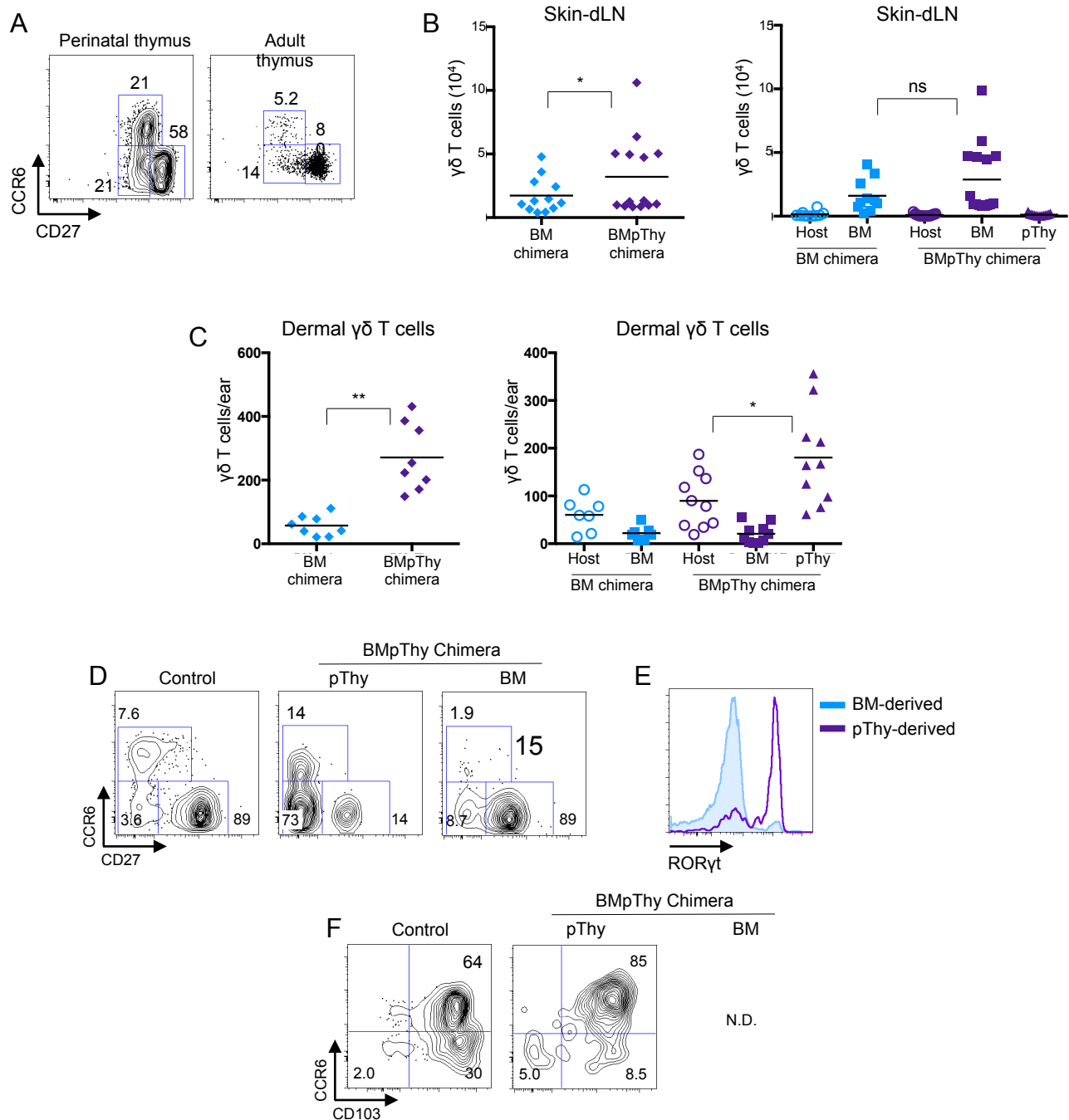


Figure 3.2. A wave of $\gamma\delta$ T cells exit the perinatal thymus (pThy) to form the circulating CCR6⁺CD27⁻ subset and dermal $\gamma\delta$ T cells. A) Perinatal (0-48hrs after birth) and adult thymus CCR6 by CD27 profiles. B-F) CD45.2⁺ TCR δ -GFP mice were irradiated and reconstituted with BM (BM only) or with BM plus pThy (BMpThy). B) Graphs show the total number of $\gamma\delta$ T cells > 8 weeks following reconstitution in the dermis and skin dLN. Geometric mean is shown. C) Contribution of BM-derived and pThy-derived $\gamma\delta$ T cells in the dermis and LN. Geometric mean is shown. D) CCR6 and CD27 profiles of $\gamma\delta$ T cells in the skin dLN and E) ROR γ t profiles of pThy and BM $\gamma\delta$ T cells in the skin dLN. F) CCR6 and CD103 profiles of $\gamma\delta$ T cells in the dermis in WT mice and naïve chimeras (N.D. = not done). Numbers denote the percentage of that population within the indicated quadrant.

dominant population in the circulation (Figure 3.2B), they failed to reconstitute the dermal $\gamma\delta$ T cell population (Figure 3.2C). In addition, the majority of $\gamma\delta$ T cells in the spleen and LN were $CD27^+$ with a minority of $CD27^-CCR6^-$ and no $CD27^-CCR6^+$ $\gamma\delta$ T cells (Figure 3.2D). Although small numbers of host $\gamma\delta$ T cells remained in the dermis following irradiation, their phenotype was abnormal and their numbers were significantly lower than in unirradiated mice (data not shown).

Importantly, $\gamma\delta$ T cell populations lost due to irradiation could be replaced by transferring perinatal thymocytes (pThy) into irradiated hosts along with congenically marked BM cells, referred to as BMpThy chimeras. This resulted in the restoration of both $CD103^+CCR6^+$ and $CD103^+CCR6^-$ dermal $\gamma\delta$ T cell populations and the circulating $CCR6^+$ population (Figure 3.2C & D). pThy also expressed high levels of ROR γ t while this was mostly absent from the BM-derived $\gamma\delta$ T cells (Figure 3.2E). Total $\gamma\delta$ T cells numbers in the dermis returned to normal levels and the phenotype of the pThy-derived dermal $\gamma\delta$ T cells resembled that of unirradiated mice (Figure 3.2F). Although pThy-derived $\gamma\delta$ T cells contributed to all three circulating populations defined by CD27 and CCR6 staining, $CD27^+$ cells were a relatively minor population.

Functional $\gamma\delta$ T cell subsets are determined independently of TCR V γ chain expression

In order to look at the distribution of V γ chain usage we used commercially available flow antibodies (V γ 1, 2, 4 and 5) to stain spleen, lymph node and skin. Of the seven V γ chain genes, $\gamma\delta$ T cells are known to utilize six (V γ 3 is excluded). Using immunofluorescence we confirmed previous reports and found high expression of V γ 5 used exclusively by DETC in the skin epidermis (Figure 3.3A & B). As a result, whole

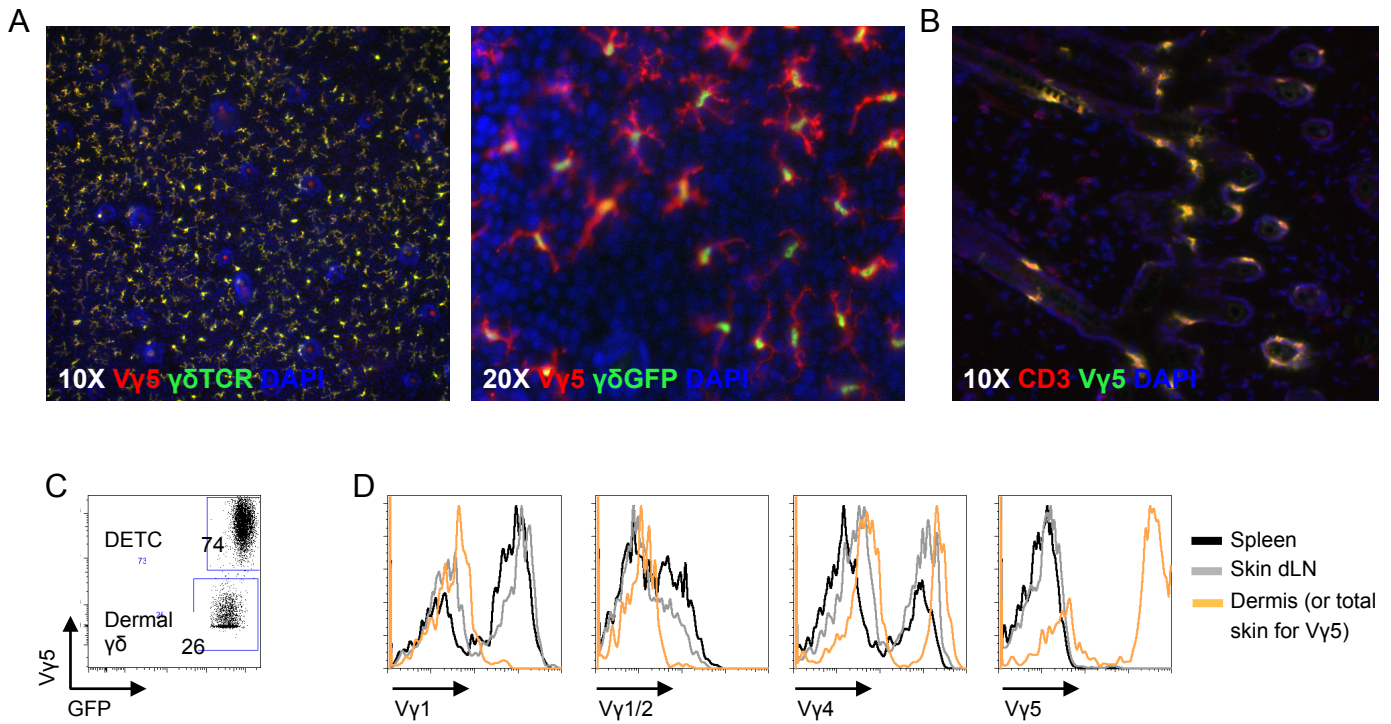


Figure 3.3. $\gamma\delta$ T cell V γ expression in the circulation and skin. A) Immunofluorescence of an epidermal peel from C57BL/6 (left) and TCR δ -GFP (right) mice and B) frozen skin cross sections from C57BL/6 mice. Samples were stained with V γ 5 (DETC-specific) and/or $\gamma\delta$ TCR as well as dapi (nucleus). C) Representative flow plot of skin demonstrating gating strategy for skin experiments. D) Representative histograms show levels of V γ 1, 1&2 and 4 expression in spleen, skin dLN and dermis. V γ 5 expression is shown for total skin.

skin was digested for flow experiments and dermal $\gamma\delta$ T cells were identified as $V\gamma 5^-$ (Figure 3.3C). In the dermis, $V\gamma 4$ is expressed by up to half of dermal $\gamma\delta$ T cells and a minority expressed $V\gamma 1$ (Figure 3.3D). In the circulation the majority were $V\gamma 1^+$ and $V\gamma 4^+$ also made up a large portion. $V\gamma 2$ is identified with an antibody that stains both $V\gamma 1$ and $V\gamma 2$, however we did not find this antibody to stain a higher proportion than $V\gamma 1$ alone, suggesting this TCR is not readily used in the circulation or dermis. Results are summarized in Table 3.1.

Considering that CD27 aligns tightly with $\gamma\delta$ T cell function, we asked whether $\gamma\delta$ T cells with a particular TCR $V\gamma$ chain favored its expression. Although it does not cover the breadth of $V\gamma$ usage, we used $V\gamma 4$ as a proxy to determine the likelihood that $\gamma\delta$ T cells with a specific function would all use the same TCR chains. We found that neither the $CD27^+$ nor $CD27^-$ populations were homogeneous populations (Figure 3.4A). Approximately 20-30% of $CD27^+$ $\gamma\delta$ T cells and 25-60% of $CD27^-$ $\gamma\delta$ T cells used $V\gamma 4$. Based on this it seems that during development, expression of CD27 is not directly tied to TCR rearrangement although perhaps $CD27^-$ $\gamma\delta$ T cells favor $V\gamma 4$.

To better address this question we also analyzed $\gamma\delta$ T cells from the thymus of adult mice and within 48 hours after birth. In the adult thymus, almost 50% of $GFP^+\gamma\delta TCR^+$ cells expressed a $V\gamma 4$ TCR and similarly, approximately 40% of total pThy were $V\gamma 4^+$ (Figure 3.4B). In the perinatal thymus, half of the $CD27^+$ population expressed $V\gamma 4$ while only a fraction of the $CD27^-$ $\gamma\delta$ thymocytes did (Figure 3.4C). In the adult thymus, all populations similarly used $V\gamma 4$. In fully reconstituted BMpThy chimeras where pThy make up a minority of $\gamma\delta$ T cells, which are mostly $CD27^-$ and

Table 3.1. $\gamma\delta$ T cell V γ genes, available antibodies and tissue localization.

Heilig & Tonegawa nomenclature	V γ 1	V γ 2	V γ 3	V γ 4	V γ 5	V γ 6	V γ 7
Commercially available Antibody	Yes	Yes*	NA	Yes	Yes	No	No
LN/Spleen	✓	X / ?	NA	✓	X	?	?
Dermis	✓ / ?	X	NA	✓	X	?	?
Epidermis	X	X	NA	X	✓	X	X

*Stains both V γ 1 & V γ 2

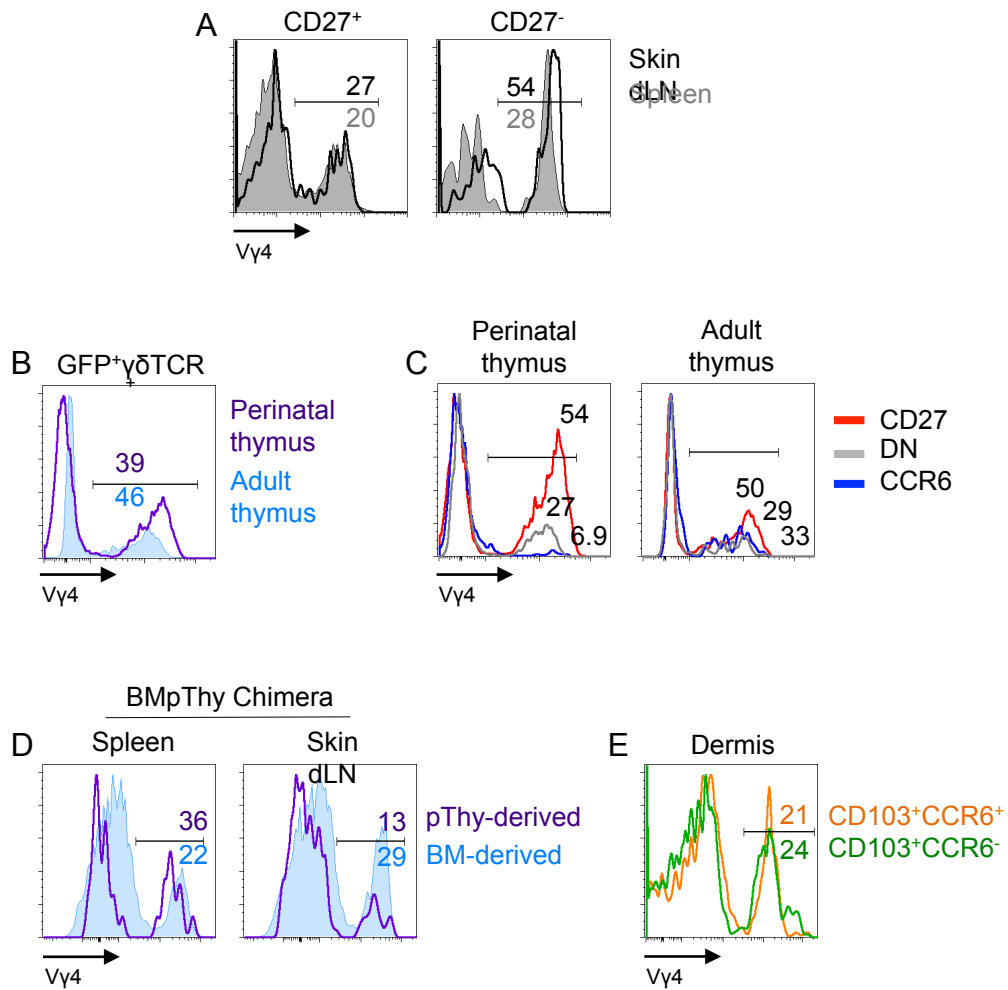


Figure 3.4. Functional $\gamma\delta$ T cell subsets are determined independently of TCR V γ chain expression. V γ 4 expression was analyzed to determine whether functional or developmental subsets were uniform in TCR usage. A) Representative histograms for CD27⁺ and CD27⁻ $\gamma\delta$ T cells in spleen and skin dLN of naïve mice. B) Total adult and perinatal thymocytes were compared for V γ 4 use. C) V γ 4 on thymocytes from perinatal (left) and adult (right) that were subsetted based on CCR6 and CD27 expression. D) V γ 4 expression on pThy-derived and BM-derived in the spleen and skin dLN from reconstituted BMpThy chimeras. Numbers denote the percentage of that population within the indicated quadrant.

BM-derived $\gamma\delta$ T cells are almost all CD27⁺, the BM- and pThy-derived $\gamma\delta$ T cells reflected similar V γ proportions (Figure 3.4D).

Although DETC within the epidermis all express an identical germline encoded TCR, dermal $\gamma\delta$ T cells do not appear to be a homogenous population. Using CD103 and CCR6 expression to identify dermal subsets, we found that 20-25% of both populations were V γ 4⁺ (Figure 3.4E). Overall this challenges the notion that $\gamma\delta$ T cells exit the thymus in strict V γ chain waves, each with a specific purpose, and instead that functional waves of $\gamma\delta$ T cells may exit the thymus that are not restricted to particular TCRs.

Discussion

One of the most challenging aspects of understanding $\gamma\delta$ T cells is a lack of context from which to study them. The $\gamma\delta$ TCR has long been the only way of identifying them, as no other marker is currently known to be unique to $\gamma\delta$ T cells. As such, TCR chain usage has been a primary method of categorizing them, but more recently it has become clear that this is possibly too simplistic and inaccurate in some cases. The most well characterized $\gamma\delta$ T cells are DETC, which follow the classical line of thought, having exited the thymus in a distinct wave with expression of a discrete TCR and entered the epidermis where they reside throughout life (50). However, it seems that this type of $\gamma\delta$ T cell population may be the exception rather than the rule, especially considering this population is not conserved across species.

The most effective way to investigate the $\gamma\delta$ T cell role in the immune system is to understand how individual cells fit within a network of fixed lineages and plastic

subsets. Recent work done by our group as well as others attempts to elucidate this system by evaluating the relationship between cell surface proteins, cell function and $\gamma\delta$ T cell development, which may still play an important role in determining their fate. CD27 is now recognized as a significant cell surface marker for $\gamma\delta$ T cells with an ability to distinguish populations fated to produce either IFN γ or IL-17 (43). Although there has been emphasis on CD27 in the circulation and its importance for determining function, less has been done to look at its expression on $\gamma\delta$ T cells in peripheral tissues such as the skin. In contrast, CCR6 is known to be expressed on $\gamma\delta$ T cells in the dermis and the associated lymphatics (34), but has not been studied well in the context of $\gamma\delta$ T cell lineages.

Here we characterize distinct subsets within the dermal and circulating $\gamma\delta$ T cell populations (Figure 3.5). CD27 delineates two independently maintained lineages of $\gamma\delta$ T cells, which remain stable in the presence of inflammation. These populations have been shown during the steady state to have distinct epigenomes (41) confirming our understanding that these are indeed separate subsets of $\gamma\delta$ T cells. Further, within the CD27⁻ population we identified two subsets based on CCR6 expression, each with unique properties. CD27⁻ $\gamma\delta$ T cells are found readily in the thymus near the time of birth and seed the circulation and dermis at this early point in development, which persist as long-lived populations. CD27⁺ $\gamma\delta$ T cells exit the thymus throughout life and contribute primarily to the circulating population where they are the majority. Although these populations are derived at different times during development, this does not necessarily correlate with TCR V γ chain expression. The dermal $\gamma\delta$ T cell population is exclusively

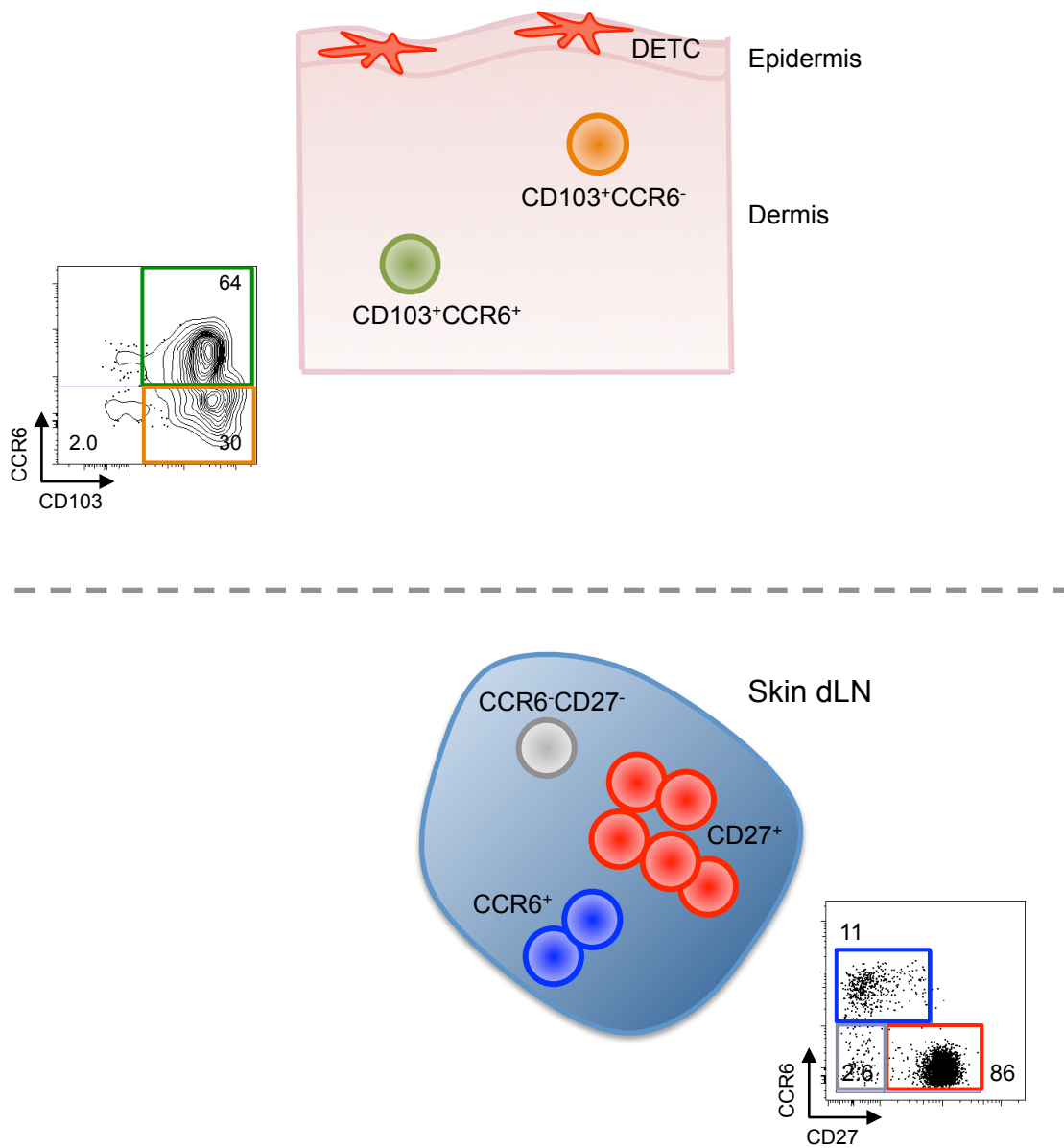


Figure 3.5. Model of $\gamma\delta$ T cell populations in the skin and skin dLN under steady state conditions.

CD27⁻ under steady state conditions and all of them are CD103⁺ with about half expressing CCR6.

Linking cell surface phenotype with TCR specificity and ultimately $\gamma\delta$ T cell function is an important avenue of research. Although the specificity of the $\gamma\delta$ TCR has remained mostly elusive, a few antigens have been identified. The most well characterized population V γ 9V δ 2-expressing $\gamma\delta$ T cells, which seem to recognize phosphoantigens and are found only in primates (51, 52). Their reliance on TCR stimulation for activation or other signals to perform effector functions is not well known, however they have potent effects on infected (53, 54) and cancerous cells (55, 56). Some V γ 9V δ 2⁺ $\gamma\delta$ T cells do express CD27 and it has been proposed that this signal integrates with TCR stimulation and contributes to their survival (45). NKG2D is another cell surface protein that has been proposed to work in concert with TCR stimulation for $\gamma\delta$ T cell activation (57, 58). It is an activating receptor, which recognizes MICA/MICB as well as ULBP molecules expressed on infected or cancerous cells (59).

Considering the limited nature of TCR expression and the variety of activating molecules on $\gamma\delta$ T cells, it is possible that even cells expressing the same TCR, V γ 9V δ 2 for example, have unique sets of co-receptors that work to fine tune alternative responses and activation requirements. This allows for a wide variety of activating requirements in the periphery and the possibility that in some cases the primary function of the TCR was during thymic development rather than recognition of foreign antigen like classical $\alpha\beta$ T cells.

Chapter 4:

Vaccinia Virus infection results in accumulation of $\gamma\delta$ T cells in the tissue
and alters the dermal $\gamma\delta$ T cell population

Introduction

Although $\gamma\delta$ T cells make up a small portion of T cells in the circulation, they are found at higher proportions in peripheral tissues such as the gut, vaginal mucosa and skin (5). While migration into tissues for $\alpha\beta$ T cells is most often in response to infection, injury or normal flora, $\gamma\delta$ T cells seem to undergo programming during development that directs them to these locations following their exit from the thymus. This hardwiring, which drives them particularly to barrier tissues such as the intestine, reproductive tract and skin, seems ideally suited to ensure that $\gamma\delta$ T cells participate in innate host defense.

While several models of systemic viral infection (60, 61) have elicited a $\gamma\delta$ T cell response in the spleen and LN, these studies did not address questions concerning tissue trafficking or provide a relevant context for natural modes of infection. Importantly, studies with human PBMC have found that $\gamma\delta$ T cells in the circulation are impacted in patients with inflammatory bowel disease (62), melanoma (63) and psoriasis (64), suggesting that local inflammation can impact global $\gamma\delta$ T cell homeostasis. These findings point to the need to understand the trafficking patterns of $\gamma\delta$ T cells during steady state conditions and in the context of disease.

In the current study, we analyzed the $\gamma\delta$ T cell response in mouse skin to local infection with Vaccinia Virus (VV). We sought to dissect the contribution of resident

versus immigrant $\gamma\delta$ T cells following infection and to determine whether $\gamma\delta$ T cells recruited from the circulation give rise to long-term residents in the skin after the cutaneous infection has cleared. Many previous reports have studied the $\gamma\delta$ T cell response in $\text{TCR}\alpha^{-/-}$ or $\text{TCR}\beta^{-/-}$ mice which lack $\text{TCR}\alpha\beta$ T cells (60, 61) or performed transfers of $\gamma\delta$ T cells isolated from $\text{TCR}\beta^{-/-}$ mice (65) to investigate the anti-viral response. In such scenarios the $\gamma\delta$ T cell makeup and response is likely abnormal (66). Analyzing $\gamma\delta$ T cells in a wild-type setting allowed us to better appreciate their role in a skin infection.

Our experiments revealed that CD27^+ and CD27^- $\gamma\delta$ T cells are specifically recruited from the circulation to the site of infection and contribute to different populations in the dermis. Surprisingly neither population becomes resident in the tissue, even when encountering a relatively empty niche.

Results

$\gamma\delta$ T cells accumulate at the site of infection with the emergence of a novel dermal population

Although it is known that $\gamma\delta$ T cells reside at barrier surfaces in mice and humans (28, 29), few studies have addressed the role they play during infection of the skin, particularly in response to viral infection. To address this, we used a model of Vaccinia VV scarification, in which virus localizes primarily to the site of inoculation (67). Following infection of the ear pinna, we observed the number of dermal $\gamma\delta$ T cells increased approximately ten-fold in the infected ear and dLN (Figure 4.1A & B). The response kinetics were slightly unusual, as the numbers in the skin and dLN remained

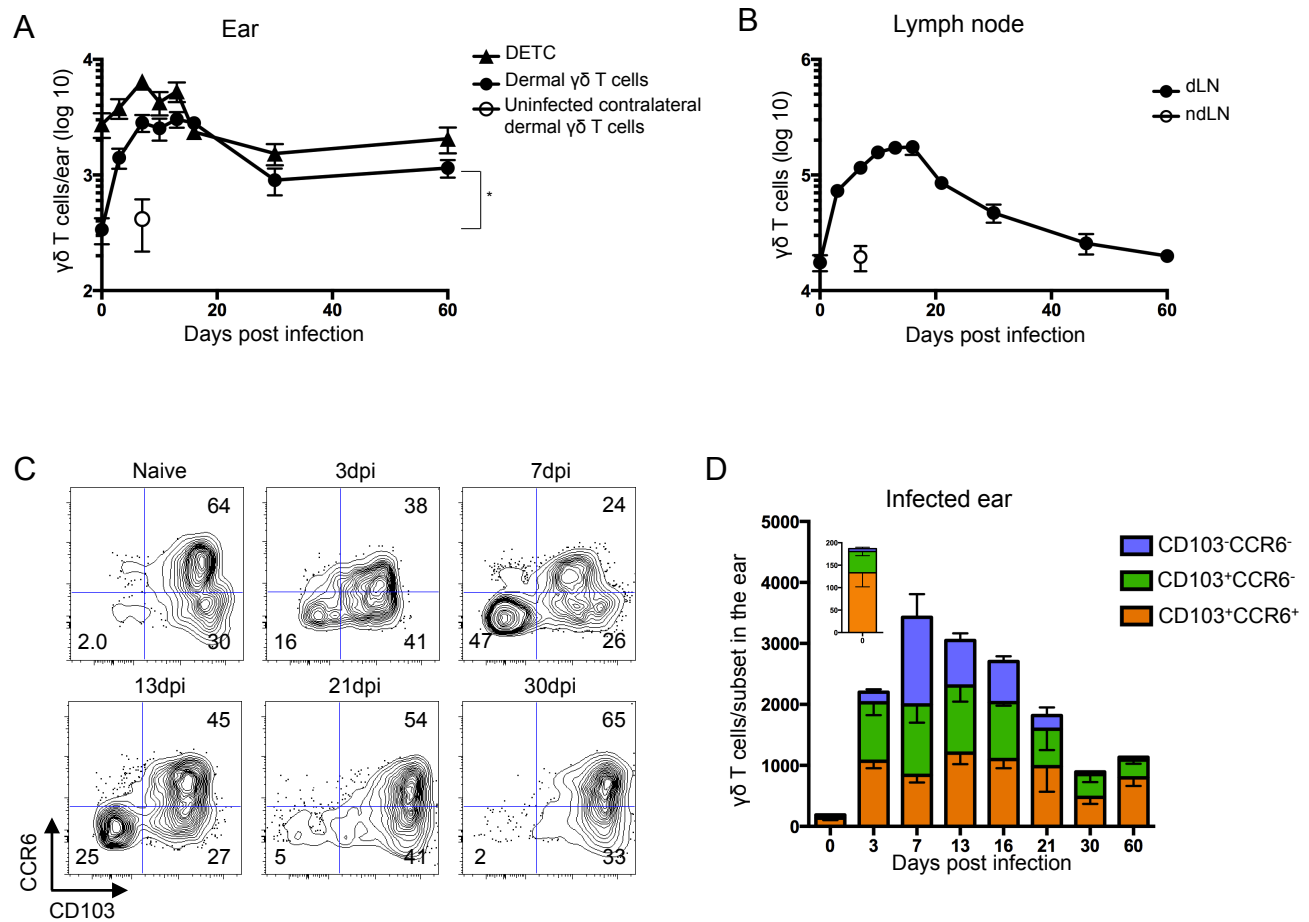


Figure 4.1. Following skin scarification with Vaccinia virus (VV), $\gamma\delta$ T cells accumulate in draining lymph node and dermis. TCR δ -GFP mice were infected with VV on the ear by scarification. $\gamma\delta$ T cells were gated as TCR β -GFP⁺ in the LN and as TCR β -GFP⁺V γ 5⁺ (Dendritic Epidermal T Cells, DETC) or TCR β -GFP⁺V γ 5⁻ (dermal $\gamma\delta$ T cells) in the ear. A) Number of DETC and dermal $\gamma\delta$ T cells in the ear following infection. Open symbol represents the number of dermal $\gamma\delta$ T cells in the contralateral uninfected ear at 7dpi. B) Number of $\gamma\delta$ T cells in the dLN following infection. Open symbol represents the number of $\gamma\delta$ T cells in the contralateral non-draining LN (ndLN) at 7dpi. C) Representative flow plots show CCR6 and CD103 profile of dermal $\gamma\delta$ T cells following infection. Numbers denote percent of total dermal $\gamma\delta$ T cell population within the indicated quadrant. D) Cell numbers within the indicated dermal $\gamma\delta$ T cell subsets over the course of infection per ear (insert, day 0). Error bars signify SEM.

elevated for a protracted period of time. Furthermore, the number of dermal $\gamma\delta$ T cells at late time points was significantly higher than in naive ears, suggesting that infection could result in prolonged alterations in the dynamics of the dermal $\gamma\delta$ T cell population. The number of DETC also increased about three-fold following infection and returned to the number found in control ears at late time points.

In resting skin, all dermal $\gamma\delta$ T cells are CD103⁺ and over half are CCR6⁺; however, skin scarification with VV resulted in dramatic changes in the dermal $\gamma\delta$ T cell population. By three days post infection, a novel subset appeared in the dermis that was CCR6 and CD103 double negative (DN) (Figure 4.1C & D). This novel dermal $\gamma\delta$ T cell subset accounted for almost half of the $\gamma\delta$ T cell population at the peak of the response, then disappeared entirely from the dermis by 30 days post infection.

Circulating $\gamma\delta$ T cells are rapidly recruited to the VV infected ear

We performed an adoptive transfer to investigate the origin of the dermal $\gamma\delta$ T cell populations following infection and to determine the contribution of circulating $\gamma\delta$ T cells to the expanded dermal population. Accordingly, 7×10^5 $\gamma\delta$ T cells isolated from the spleen and skin dLN of naïve TCR δ -GFP mice were transferred intravenously into normal C57BL/6 recipients before VV scarification. Infection of the recipients showed that donor $\gamma\delta$ T cells were specifically recruited to the skin of the infected ear and their numbers peaked 7 days post infection (Figure 4.2A). While these adoptively transferred, circulating cells were capable of entering the dermis during active infection, very few remained permanently integrated into the dermis at a late time point.

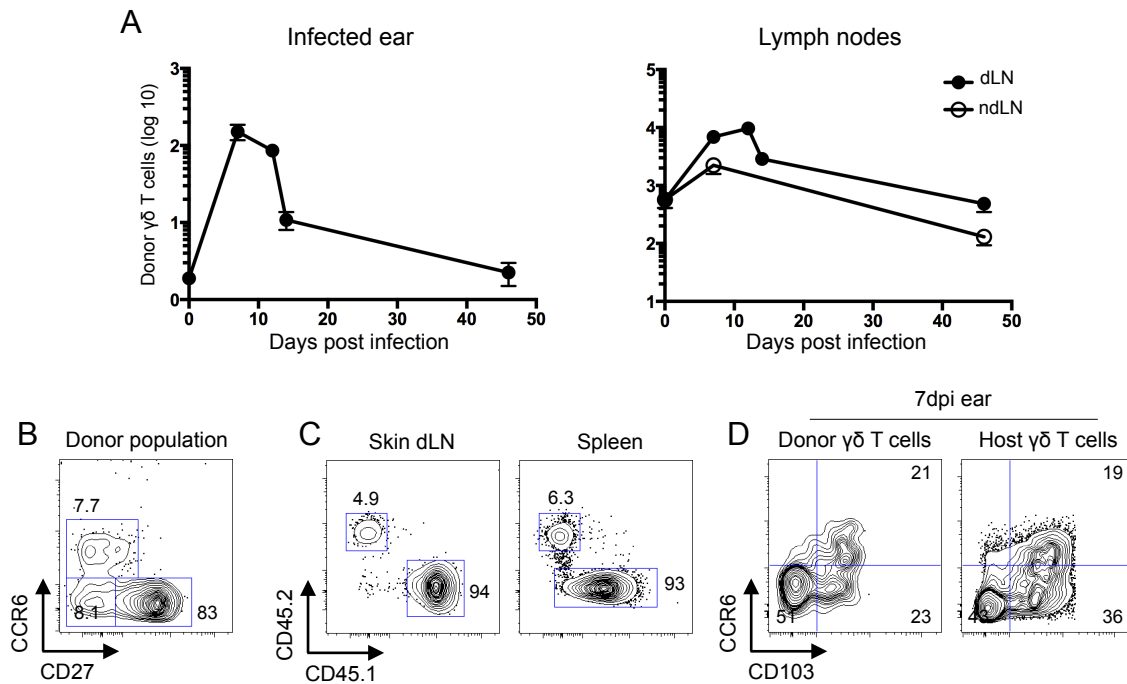


Figure 4.2. Circulating $\gamma\delta$ T cells migrate to VV infected skin and contribute to all three dermal subsets. C57BL/6 mice (CD45.2) or CD45.2⁺ TCR δ -GFP mice received 7×10^5 $\gamma\delta$ T cells isolated from spleen and skin dLN of CD45.1⁺ TCR δ -GFP mice. The following day, mice were infected with VV on the ear. A) Graphs show numbers of transferred TCR δ -GFP⁺ cells recovered from the LN or ear, shown as \pm SEM. B) Representative flow plot shows the CCR6 and CD27 profile of the donor $\gamma\delta$ T cell population prior to transfer. C) Representative flow plots showing the proportion of donor (CD45.2) to host (CD45.1) in the skin dLN and spleen 1 day post transfer. D) Representative flow plots show CCR6 and CD103 profile of donor and recipient dermal cells at 7dpi.

The donor population accurately reflected the typical makeup of circulating $\gamma\delta$ T cell proportions (Figure 4.2B) and made up 5% of the total $\gamma\delta$ T cell population in the spleen and LNs before infection (Figure 4.2C). Transfer experiments revealed that the donor $\gamma\delta$ T cells contributed to all three dermal $\gamma\delta$ T cell populations defined by CD103 and CCR6 staining (Figure 4.2D), but it was not clear how these populations related to those in the circulation.

Our initial attempts to stain for CD27 on $\gamma\delta$ T cells isolated from the ear were negative. Further analysis revealed that CD27 was cleaved during the digestion process used to isolate cells from the ear (Figure 4.3A). Floating ears (dorsal and ventral sides separated) overnight in complete media without enzymatic digestion released some $\gamma\delta$ T cells from the tissue and permitted analysis of CD27 expression (Figure 4.3B). Although CD27⁺ $\gamma\delta$ T cells predominate in the circulation, none were found in naïve dermal tissue.

Using this technique with infected samples revealed that although CD27 was not found on dermal $\gamma\delta$ T cells in naïve animals, it was expressed on some dermal $\gamma\delta$ T cells following infection, all of which belonged to the CD103⁻CCR6⁻ DN population (Figure 4.3C). This suggested that the CD103⁻CCR6⁻ DN subset appearing in infected ears was an immigrant population of circulating CD27⁺ $\gamma\delta$ T cells. Because yields and subset composition from the floating technique were variable, we opted to use CD103 and CCR6 for further analyses of skin samples.

To ask whether CD27⁺ or CD27⁻ $\gamma\delta$ T cells from the circulating pool differentially contributed to the three dermal $\gamma\delta$ T cell subsets, we sorted and transferred them into separate hosts before ear scarification with VV. The CD27⁻ donor $\gamma\delta$ T cells contributed

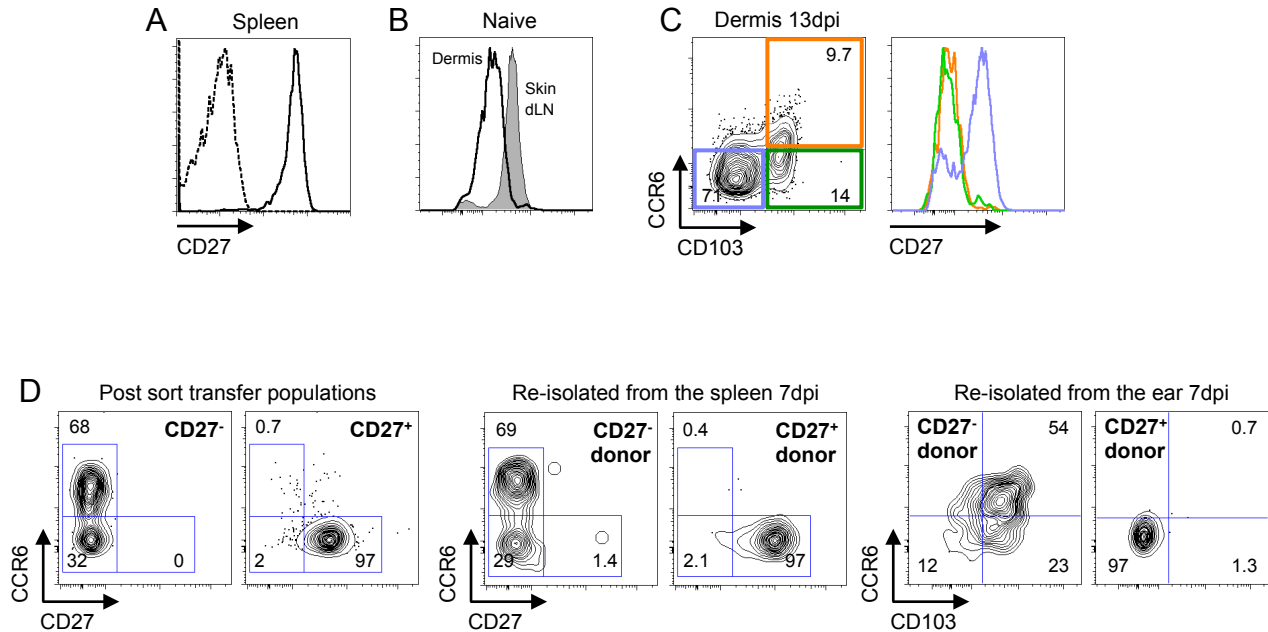


Figure 4.3. CD27⁺ $\gamma\delta$ T cells are only found in inflamed skin and contribute specifically to the CD103⁻ dermal population. A) Representative flow plot of CD27 expression on $\gamma\delta$ T cells from spleen samples treated with liberase (dashed line) or left untreated (solid line). B) To avoid liberase digestion of skin, naïve ears were floated in media overnight. Representative flow plot of CD27 expression on dermal $\gamma\delta$ T cells (black line) released from the tissue by floating and skin dLN (grey filled). C) CD27 staining on dermal $\gamma\delta$ T cells floated from 13dpi infected ears without enzymatic treatment. D) $\gamma\delta$ T cells from spleen and skin dLN of TCR δ -GFP mice were sorted based on CD27 expression and 6×10^5 CD27⁺ or 2.7×10^5 CD27⁻ $\gamma\delta$ T cells were transferred into separate C57BL/6 mice. Recipients were infected with VV on the ear the following day. Flow plots show the phenotype of CD27⁻ and CD27⁺ at the time of transfer and 7dpi in the spleen and ear. Numbers denote the percentage of cells within the indicated quadrant. Data are representative of at least two independent experiments, n=3-7 mice per group.

to all three dermal populations defined by CD103 and CCR6, although few were DN and most expressed CD103 (Figure 4.3D). In contrast, immigrant $\gamma\delta$ T cells from the CD27⁺ donor population were exclusively CD103⁻CCR6⁻ DN, even though 50% of cells in the donor population expressed CD103. On a per cell basis, the CD27⁻ $\gamma\delta$ T cells were recruited more efficiently to the infected skin.

$\gamma\delta$ T cells show limited proliferation following infection

In addition to recruitment, we wanted to know whether the changes we saw in the number of $\gamma\delta$ T cells could be due to proliferation. To do this we took several approaches commonly used to assess cell proliferation. Ki67 is a protein strictly expressed in all cells undergoing division (68), therefore we stained the dLN and skin at day 3 post infection when the cell numbers start to increase. Although staining was above background (determined by an isotope control antibody), there was no difference between naïve and infected samples in any of the populations by percent in the skin dLN or dermis (Figure 4.4A & B). The total number of $\gamma\delta$ T cells is higher at day 3 and so there might be slightly more total Ki67⁺ cells in the infected samples, but the vast majority of cells are not undergoing active proliferation by this method of detection at this time point when we see $\gamma\delta$ T cell accumulation in these tissues.

We next assessed proliferation with Bromodeoxyuridine (BrdU), which is incorporated into the DNA of replicating cells. Depending on the length of time, delivery method and amount of BrdU in the animal, a window of proliferation is captured. We chose to inject mice on day 3 or day 5 post infection with BrdU 1 hour before tissues were harvested to determine how much proliferation is occurring over a short period of

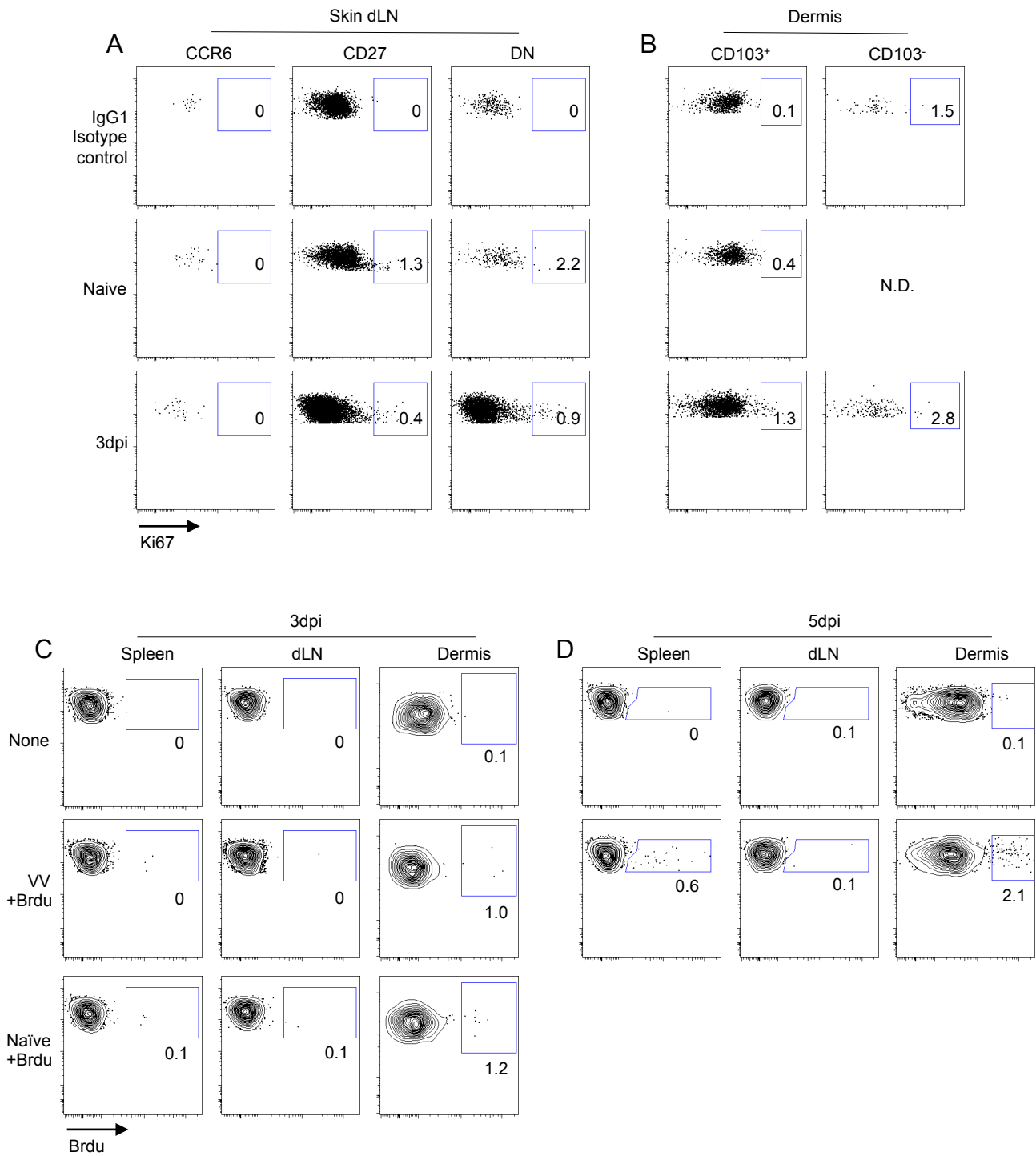


Figure 4.4. Low level of $\gamma\delta$ T cell proliferation in situ following VV infection. Representative flow plots of Ki67 expression in $\gamma\delta$ T cells in the A) dLN (or skin dLN for naïve) and B) dermis of naïve and 3 day infected mice (N.D. = no data). $\gamma\delta$ T cell Brdu incorporation after 1 hour on C) day 3 and D) day 5 post infection in the spleen, skin dLN and dermis. Numbers indicate percent of total population.

time and exactly in what location. These results confirmed what we saw with Ki67 that very little proliferation is happening at day 3 (Figure 4.4C), however by day 5 Brdu incorporation could be seen in the dermis and to a lesser extent the spleen (Figure 4.4D). Proliferation in the dermis over a short period of time suggests that dermal $\gamma\delta$ T cells are expanding within the tissue.

The last method we used is one commonly applied to antigen-specific $\alpha\beta$ T cells whereby cells are isolated, stained with a dye (CTV used here) that enters the cytoplasm of cells and transferred into a new host. The most brightly stained cells are undivided and at each cell division the dye is halved, resulting in a series of fluorescent peaks. By day 7 post infection, very few cells had diluted the CTV (Figure 4.5). This further indicates that very little proliferation among circulating $\gamma\delta$ T cells has occurred in response to infection by the peak of the response. Together this data supports the notion that a fraction of dermal $\gamma\delta$ T cells proliferate and the majority of $\gamma\delta$ T cells in circulation migrate to the site of infection and dLN.

Adult BM- and pThy-derived $\gamma\delta$ T cells occupy discrete niches

We have established that BMpThy chimeras allow us to identify circulating (BM-derived) and resident dermal (pThy-derived) $\gamma\delta$ T cells by taking advantage of when each population exists the thymus. Using BMpThy chimeras, we confirmed that, following VV infection, adult BM-derived $\gamma\delta$ T cells (largely CD27⁺ in the circulation) were transiently recruited from the circulation and contributed primarily to the CCR6⁻ CD103⁻ DN dermal subset (Figure 4.6A & B).

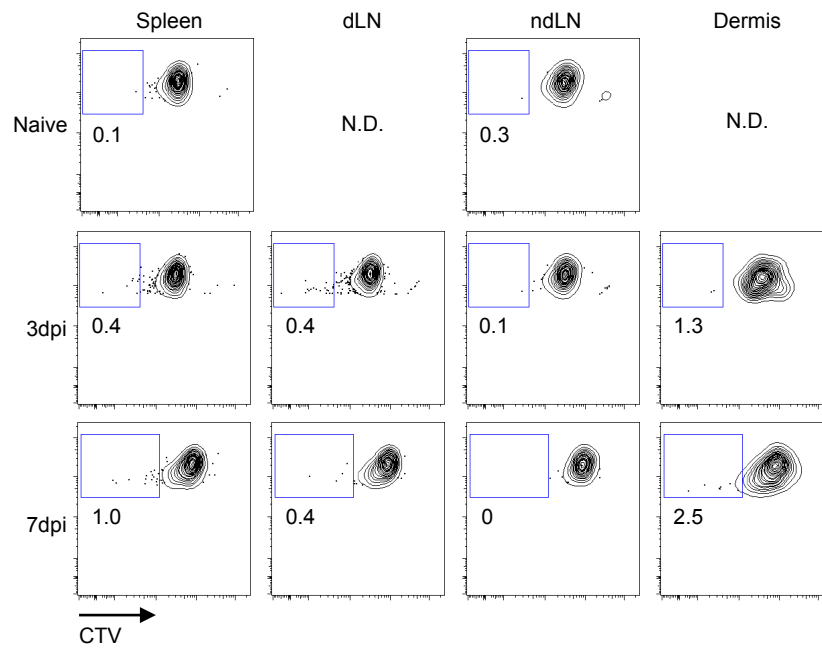


Figure 4.5. Low level of transferred $\gamma\delta$ T cell proliferation and accumulation in vivo following VV infection. Representative flow plots of CTV dilution in $\gamma\delta$ T cells in the spleen, dLN, ndLN and dermis. Cells were harvested from skin dLN and spleen of TCR δ -GFP mice, labeled with CTV and transferred one day before infection. Gated on live cells. Numbers indicate percent of total population.

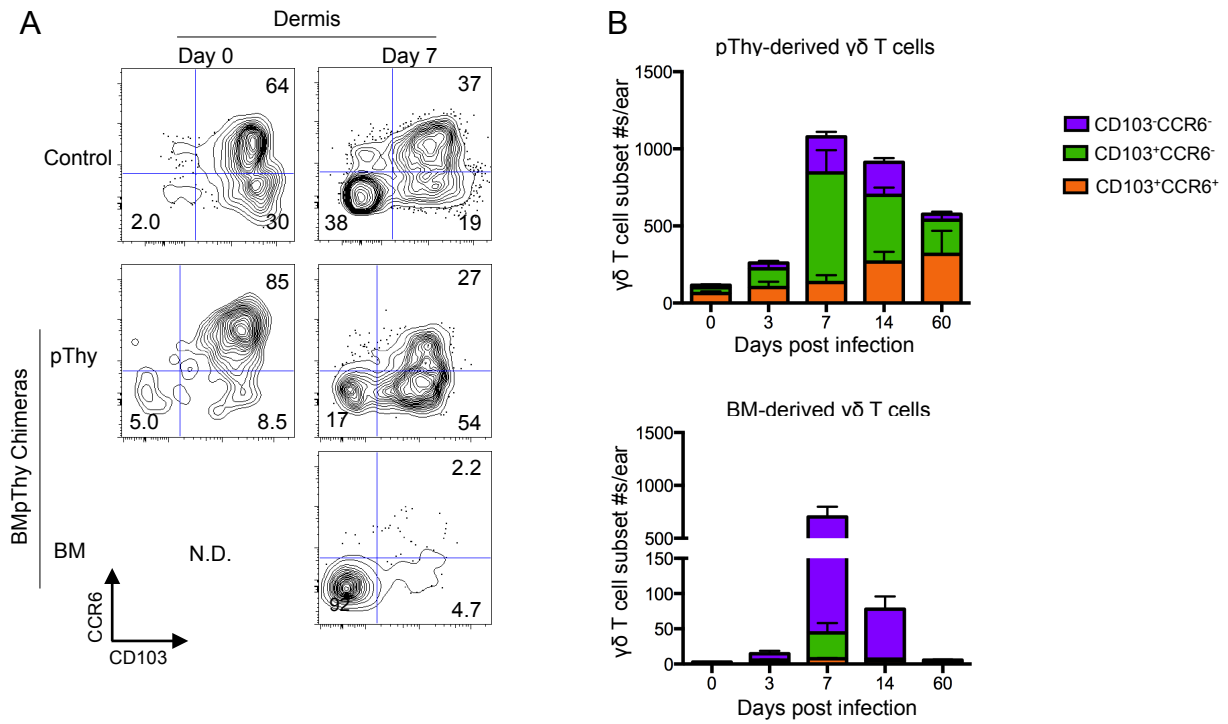


Figure 4.6. Contribution of adult BM-derived and perinatal thymus-derived $\gamma\delta$ T cells to the dermal response. CD45.2⁺ TCR δ -GFP mice were irradiated and reconstituted with BM (BM only) or with BM plus pThy (BMpThy). BMpThy chimeras were infected with VV on the ear > 8 weeks following reconstitution. A) CCR6 and CD103 profiles of $\gamma\delta$ T cells in the dermis at day 0 and 7dpi (N.D. = not done). Numbers denote the percentage of that population within the indicated quadrant. B) The number of BM- and pThy-derived $\gamma\delta$ T cells contributing to subsets in the dermis following infection. Error bars signify SEM. Statistics performed with the two-tailed, unpaired student *t*-test, **p*<0.02, ***p*<0.0001, NS = not significant. Data show results >2 independent experiments, n=3-15 mice per group.

In contrast, resident dermal pThy-derived $\gamma\delta$ T cells contributed mainly to the two CD103⁺ subsets in the dermis and their expansion during infection. As early as day 3 following infection, pThy-derived $\gamma\delta$ T cells had expanded in the dermis and their numbers remained elevated for a protracted period of time (Figure 4.6B). In contrast, the number of the BM-derived $\gamma\delta$ T cells peaked at 7 days post infection and then declined dramatically. Importantly, at a late time point the BM-derived $\gamma\delta$ T cells were absent from the ear while the pThy-derived $\gamma\delta$ T cells plateaued at a level similar to wild type (WT) mice following infection. This suggests that while immigrant $\gamma\delta$ T cells are not able to join the resident dermal population, the existing dermal population may expand and be permanently altered following infection.

Discussion

A challenge to studying $\gamma\delta$ T cells is that their numbers are very small in the circulation of mice. To get around this, several groups have used TCR β ^{-/-} mice so that the only T cells in the mouse express the $\gamma\delta$ TCR (60, 61, 65). However, this only forces the thymus to create a full T cell repertoire with different genes and does not simply remove one cell type. It has been shown that doing so alters the $\gamma\delta$ T cell makeup and their response to infection is likely abnormal (66). We chose to perform all experiments analyzing $\gamma\delta$ T cells from WT mice, including all transfers experiments. In this way $\gamma\delta$ T cells developed under normal constraints in a full compartment.

The fact that $\gamma\delta$ T cells are found more readily in tissues, however, led us to use a model that was perhaps more relevant to their function. VV is used as a vaccine for smallpox as it is a less severe form of the disease. Administration of the vaccine is done

by skin scarification with a bifurcated needle, which is the virus' natural mode of transmission (69, 70). Although one study looked at the $\gamma\delta$ T cells response to VV (61), it was following a very high dose via the intraperitoneal route of infection, which does not accurately portray viral spread or cell trafficking.

Following scarification with VV, we found that $\gamma\delta$ T cells accumulate in the dermis of the infected ear and the corresponding dLN. DETC also expanded to some extent and this is the first time, to our knowledge, of documentation of their response to viral infection of the skin. In addition to the expansion of the resident CD103⁺ populations, we noticed the presence of a novel CD103⁻ population that appeared within a few days of infection and peaked around day 7. Although it constituted half of the $\gamma\delta$ T cells in the dermis at the peak, this population was not found at a memory time-point. Interestingly, the total number of dermal $\gamma\delta$ T cells remained elevated for a prolonged period of time before declining. At a memory time-point there were significantly more dermal $\gamma\delta$ T cells, suggesting that infection permanently altered the population. Our limited understanding of the adaptive properties of $\gamma\delta$ T cells makes it difficult to assess whether this is a form of 'memory', but the change in total number suggests some capacity for modification in response to a pathogen.

Considering the appearance of a new population we asked whether any of the three populations in the inflamed ear were derived from the circulation. Transferring $\gamma\delta$ T cells first revealed that the dermal population is independently maintained from those in the circulation as they did not enter the dermis of naïve mice, which has been demonstrated previously in the gut (8). Importantly, following infection the transferred population specifically entered the infected ear. It was interesting to find that the

transferred $\gamma\delta$ T cells that entered the dermis had a similar phenotype to the total host population, supporting the notion that a large number of the $\gamma\delta$ T cells in the dermis during infection have been recruited. Further supporting this, we tested several methods of assessing proliferation and found that overall $\gamma\delta$ T cells did not readily undergo cell division. The most we were able to observe was by Brdu, which revealed local proliferation of dermal $\gamma\delta$ T cells within the tissue.

Finally, we used BMpThy to demonstrate different roles for the circulating vs. resident dermal $\gamma\delta$ T cells during infection. pThy-derived $\gamma\delta$ T cells, which dominate in the dermis, expand and contribute largely to the CD103⁺ population. BM-derived $\gamma\delta$ T cells expand in the circulation and enter the dermis, peaking at day 7 post infection. Confirming results obtained with the transfer experiments, largely CD27⁺ BM-derived $\gamma\delta$ T cells made up the DN dermal population.

Using an infectious model to investigate $\gamma\delta$ T cell population dynamics uncovered previously unappreciated ways of looking at $\gamma\delta$ T cells in the dermis and circulation. We originally thought that CD103 clearly distinguished between resident and immigrant $\gamma\delta$ T cells in the dermis during an inflammatory state. Further experiments revealed that it was not so straightforward because circulating $\gamma\delta$ T cells were able to contribute to all three populations – while all CD103⁻ $\gamma\delta$ T cells are immigrants, not all CD103⁺ are resident. Another way of looking at these populations is by CD27 expression. CD27⁺ $\gamma\delta$ T cells exclusively contribute to the CD103⁻ population, however while the majority of CD27⁻ $\gamma\delta$ T cells were CD103⁻ in the dermis, a few were found in the CD103⁻ compartment. Considering these cells are all CCR6 we conclude that these few CD27⁻ CD103⁻ $\gamma\delta$ T cells, which are capable of producing IL-17, came from the circulating

CCR6⁻CD27⁻ population. Lastly, a wave of $\gamma\delta$ T cells exists in the thymus near the time of birth that become CCR6⁺CD27⁻ or CCR6⁻CD27⁻ in the circulation and fill the dermal compartment. It seems that although the circulating population does not enter the skin during the steady state, these cells are rapidly recruited to the skin following infection and for the most part resemble resident dermal $\gamma\delta$ T cells – a subset they likely emigrated into the periphery with.

Considering how inflammation impacts the $\gamma\delta$ T cell network in the dermis, we have created new terminology that temporarily applies to dermal $\gamma\delta$ T cells during this state. Since CD103 does delineate the appearance of a novel population, CD103⁻ designates “inflammatory recruited $\gamma\delta$ T cells” and CD103⁺ designates “inflammatory resident $\gamma\delta$ T cells”. The inflammatory recruited population is entirely made up of $\gamma\delta$ T cells that have come from the circulation and will not remain long term. All of them are CCR6⁻ and the majority is CD27⁺. This population can be derived from the BM although some may be restricted to a pThy wave. Within the inflammatory resident population are a mixture of permanent resident dermal $\gamma\delta$ T cells and some that have been recruited from the circulation. All are CD27⁻, are derived from the pThy wave and approximately half express CCR6. Transfer studies support the notion that even these recruited cells will not stay long term, but the original dermal $\gamma\delta$ T cell population may expand and leave behind some of those generated during infection.

Chapter 5:

Function and role of inflammatory resident and recruited $\gamma\delta$ T cells

Introduction

The most well defined function of $\gamma\delta$ T cells is their ability to rapidly produce cytokines during the early stages of infection, before the initiation of the $\alpha\beta$ T cell response (3). A portion of them, now known to be CD27⁻, produce IL-17 (28, 30, 33, 71, 72) while the majority, which express CD27, are IFN γ -producers (73). Because of their ambiguous nature, many approaches have been taken to determine the role of $\gamma\delta$ T cells. As a result they appear to be a jack-of-all-trades, capable of performing a wide variety of functions. Previous studies attribute them with the ability to perform antigen presentation (74-79), enhance CD8⁺ T cell priming via dendritic cell maturation (80), boost CD8⁺ T cell memory formation (81), recruit neutrophils (28, 32, 59, 71, 82) and many other roles that are critical to the anti-viral response. We therefore sought to determine whether $\gamma\delta$ T cells were performing any of these or other functions during VV infection.

Considering the close relationship between $\gamma\delta$ T cell development, localization and phenotype, we also wanted to determine whether populations derived at different periods throughout life had distinct functions during infection. BMpThy chimeras previously revealed that BM- and pThy-derived $\gamma\delta$ T cells occupy distinct niches in the circulation and dermis. Further, they uniquely contribute to the different inflammatory dermal populations, making it an ideal system to assess the relationship between development and function in an infectious setting. This system also allows us to further

probe whether the inflammatory resident or recruited populations serve unique functions in the anti-viral response.

Results

Loss of $\gamma\delta$ T cells does not impact inflammatory cytokine production in the tissue

In order to assess whether the presence of $\gamma\delta$ T cells in the tissue affects the cytokine milieu, we used a CBA kit to measure the levels of six cytokines associated with inflammation: IL-6, IL-10, MCP-1, IFN γ , TNF and IL-12p70. C57BL/6 or TCR $\delta^{-/-}$ mice were infected with VV scarification on the ear and tissues were harvested at 24 hour intervals through day 4. At various time points following infection, tissue from the TCR $\delta^{-/-}$ mice had higher levels of several cytokines, namely MCP-I, TNF and IL-12p70; however these differences were not significant (Figure 5.1).

$\gamma\delta$ T cells do not significantly impact the antigen specific CD8⁺ T cell response or resolution of infection

Since it has been suggested that $\gamma\delta$ T cells may directly or indirectly impact CD8⁺ T cells during infection (80, 81), we assessed the total number of antigen specific CD8⁺ T cells at the peak of the response. To do this we transferred OT-I cells, which are specific for OVA (SIINFEKL peptide), into WT and TCR $\delta^{-/-}$ mice and infected them with VV expressing OVA. We found no difference in the number of OT-I in the infected ear 7 days post infection (Figure 5.2A).

We took two approaches to determine how the loss of $\gamma\delta$ T cells would impact viral load and we also wanted to confirm that scarification did indeed produce a

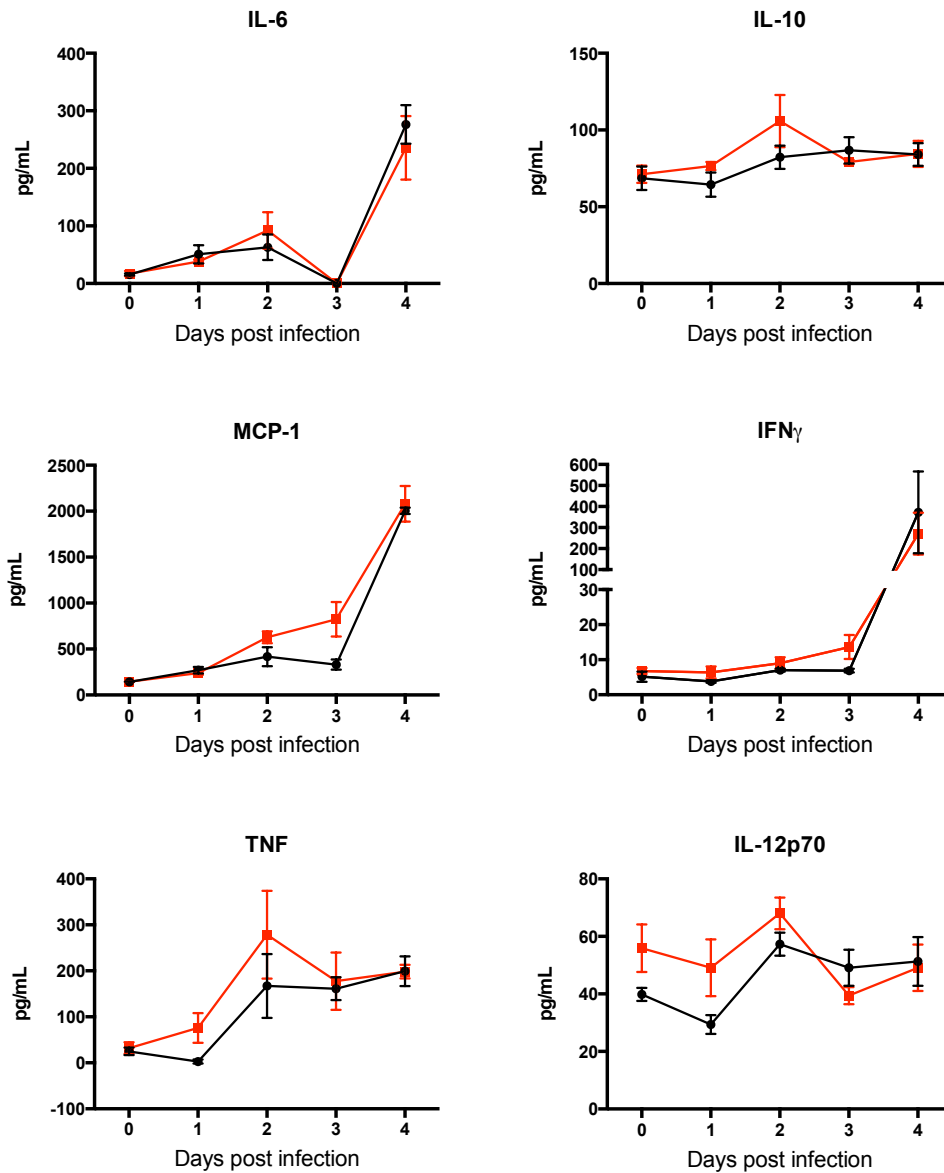


Figure 5.1. Cytokine production in the ear following VV scarification. WT (black) and TCR $\delta^{-/-}$ (red) mice were sacrificed at the indicated time points following infection and ears were processed then stained with a CBA kit to determine levels of each cytokine. SEM is shown. N=3 mice per group.

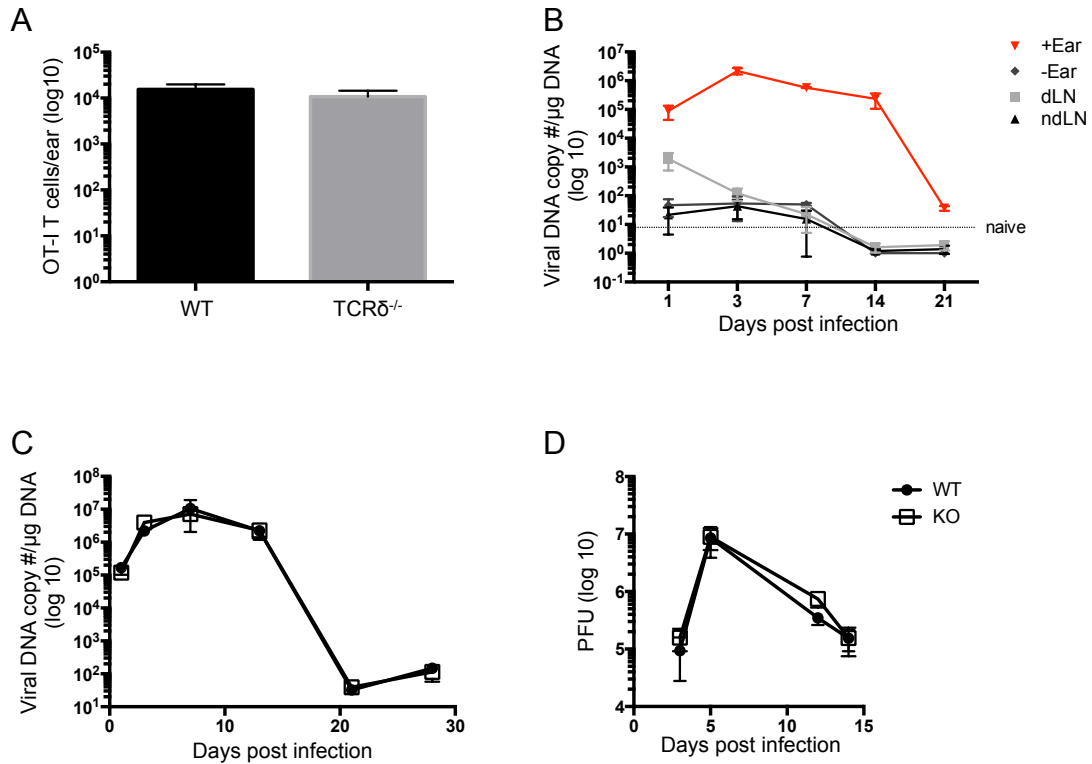


Figure 5.2. Loss of $\gamma\delta$ T cells does not impact antigen specific CD8 T cell response or viral load. A) Number of OT-I T cells in the ear of WT (black) and TCR $\delta^{-/-}$ (grey) mice at 7 days post infection. B) VV infected ear (+Ear), corresponding dLN, contralateral control ear (-Ear) and corresponding ndLN were harvested at the indicated time points following infection and analyzed by qPCR for viral DNA. C and D) VV infected ears from WT (solid circle) and TCR $\delta^{-/-}$ (open square) mice were analyzed by C) qPCR and D) plaque assay to determine viral titer at the site of infection. N=3-6 mice per group.

localized infection with limited dissemination. WT mice were scarified with VV and the infected ear, contralateral control ear and their corresponding dLNs were harvested and analyzed by qPCR. Confirming previous reports, the majority of viral DNA was found in the infected ear with perhaps a small amount in the dLN and almost none in the contralateral tissues (Figure 5.2B).

We next compared VV DNA levels in the infected ears of WT and TCR^{-/-} mice and found no difference at any time point (Figure 5.2C). Since viral DNA remained for a long period of time after live virus is presumably cleared from the mouse, we turned to plaque assay for more sensitive analysis. Using this method we again found no viral spread to the dLN or other tissues (data not shown) in WT or TCR^{-/-} mice and no difference in the viral load over the course of infection (Figure 5.2D). Therefore we concluded that $\gamma\delta$ T cells are not necessary for VV containment or clearance.

Inflammatory resident and recruited $\gamma\delta$ T cells are functionally distinct

Several groups have established that dermal $\gamma\delta$ T cells are fated to produce IL-17 (28, 33, 72). We found that a fraction of dermal $\gamma\delta$ T cells in uninfected ears produced this cytokine following *in vitro* stimulation with PMA/Ionomycin (Figure 5.3A). On day 3 after VV scarification, CD103⁺ $\gamma\delta$ T cells in the dermis were capable of producing IL-17 at a level similar to that of naïve tissue. Although they represented a minority at day 3, it was surprising that CD103⁻ $\gamma\delta$ T cells also produce IL-17 in the dermis. Using the float method in order to preserve CD27 expression, we found that all the IL-17 production was by CD27⁻ $\gamma\delta$ T cells (Figure 5.3B), which we predict are derived from the circulating CCR6⁻CD27⁻ population.

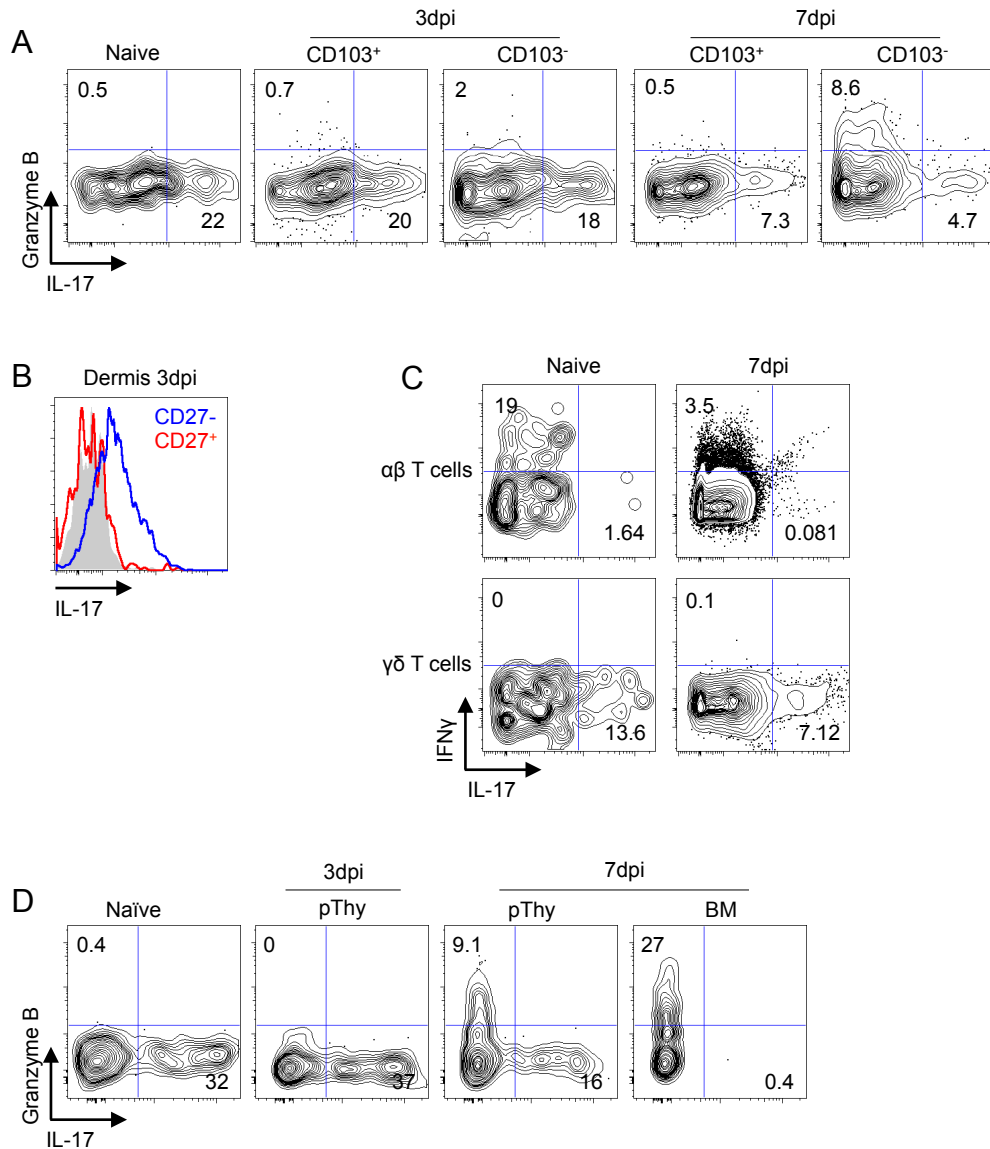


Figure 5.3. Adult BM-derived and pThy-derived $\gamma\delta$ T cells in the dermis are functionally distinct. A) TCR δ -GFP mice were infected with VV on the ear and sacrificed on days 3 and 7. Ears were digested in Brefeldin A and cells were re-stimulated with PMA/Ionomycin for 4 hours at 37°C followed by intracellular staining for cytokines and Granzyme B. Representative flow plots are shown and gates are based on unstimulated naïve samples. Numbers indicate the percentage of that population in each quadrant. Data are representative of at >2 independent experiments. B) Cytokine staining of dermal $\gamma\delta$ T cells isolated from day 3 infected ears by flotation in complete medium. IL-17 production by CD27⁺ (blue) and CD27⁻ (red) $\gamma\delta$ T cells. Gated on CD103⁻ dermal $\gamma\delta$ T cells. Gray histogram is unstimulated naïve control. C) Cytokine staining for IL-17 and IFN γ in $\alpha\beta$ versus $\gamma\delta$ T cells in the dermis of TCR δ -GFP mice 7dpi. D) BmpThy were infected and analyzed as in A).

Notably, there were no Granzyme B⁺ $\gamma\delta$ T cells in the naïve dermis at day 3 post infection, but by day 7 (which is the peak for the immigrant population), the CD103⁻ $\gamma\delta$ T cells produced Granzyme B (Figure 5.3A). Although CD27⁺ $\gamma\delta$ T cells from the naïve circulation, which make up a majority of the CD103⁻ population in the dermis, are readily capable of producing IFN γ , none of the $\gamma\delta$ T cells in the dermis stained positive for IFN γ at any time following VV scarification (Figure 5.3C).

We repeated these intracellular staining experiments with BMpThy chimeras to determine whether the BM- and pThy-derived populations had distinct functions. At day 3 post infection, there were too few BM-derived cells to be analyzed, but the pThy-derived $\gamma\delta$ T cells readily produced IL-17 (Figure 5.3D). By day 7 post infection, a clear distinction between the two populations could be seen, demonstrating that in this infection model, the function of adult BM-derived $\gamma\delta$ T cells from the circulation was to make Granzyme B while the dermal pThy-derived $\gamma\delta$ T cells gave rise to a population capable of making either IL-17 or, to a lesser extent, Granzyme B.

Resident dermal $\gamma\delta$ T cells enhance the early immune response to infection

To determine whether $\gamma\delta$ T cells contributed to inflammation, we assessed tissue pathology in wild type (WT) and TCR δ ^{-/-} mice, which lack all $\gamma\delta$ T cells. By 3 days post infection, WT ears had evidence of both epidermal and cartilage necrosis, often with entire sections of the epidermis replaced by serocellular crusts (Figure 5.4A). The dermis of these mice predominantly contained accumulation of intact and degenerate neutrophils along with some macrophages and fewer lymphocytes. In contrast, there was less infiltration of neutrophils and macrophages in the ears of TCR δ ^{-/-} mice and the

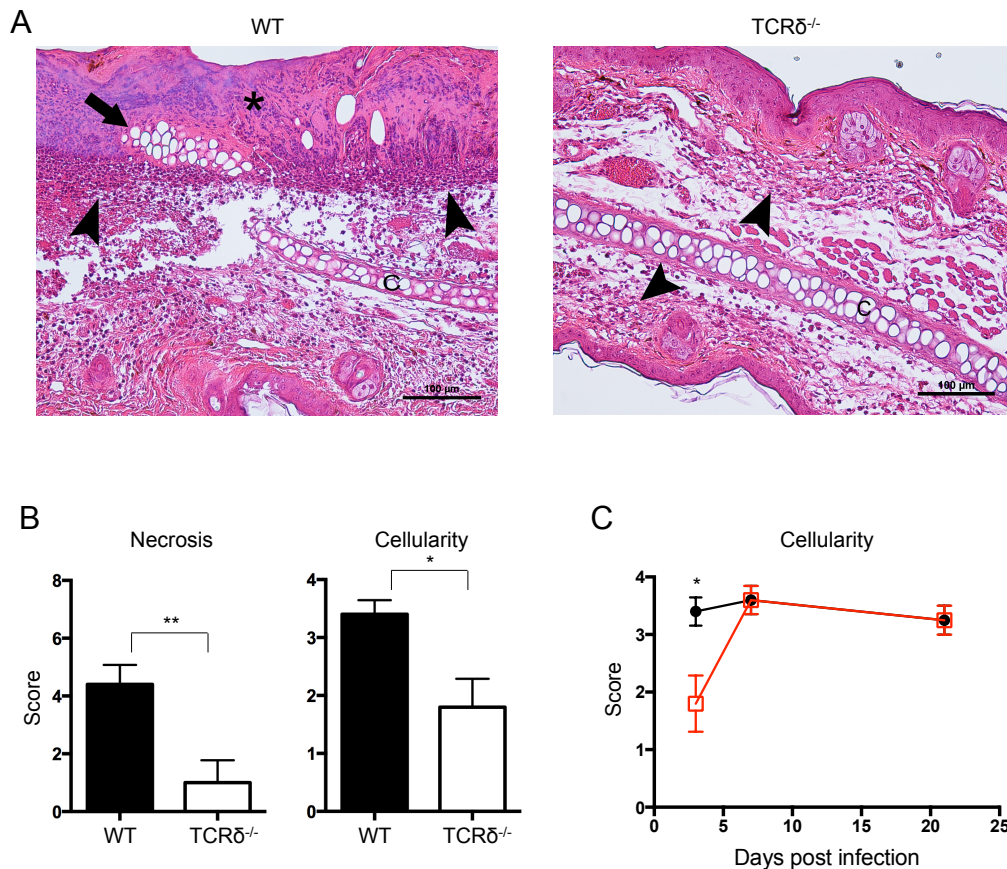


Figure 5.4. Absence of $\gamma\delta$ T cells reduces tissue pathology during VV infection. Mice were infected with VV on the ear. A) Representative histological sections of ears from C57BL/6 WT and TCR $\delta^{-/-}$ mice 3dpi at 40x magnification. Arrows indicate necrotic cartilage, arrowheads indicate neutrophilic infiltrates and asterisks indicate serocellular crusts. B) Graphs show scores for necrosis (epidermis and cartilage scored separately and then combined) and cellularity. Mean \pm SEM is shown. C) Graph of cellularity score over time for WT (black) and TCR $\delta^{-/-}$ (red). Statistics performed with the two-tailed, unpaired student *t*-test, $n=5-6$ mice per group. * $p<0.05$, ** $p<0.01$, *** $p<0.005$ Data are representative of >1 independent experiments, $n=3-6$ mice per group (C) or >2 (A, B) independent experiments, $n=5-6$ mice per group.

cartilage and epidermis remained largely intact. Comparing the histological analysis for necrosis (combined for epidermis and cartilage) and cellularity, WT mice scored significantly higher than TCR $\delta^{-/-}$ mice (Figure 5.4B). By day 7 post infection and for later time points both groups had similar scores for cellularity (Figure 5.4C) and the same pattern was seen for necrosis (data not shown).

We next compared the histologic changes of BMpThy chimeras and BM chimeras to determine whether the differences between WT and TCR $\delta^{-/-}$ mice could be assigned to the presence or absence of resident dermal $\gamma\delta$ T cells. By and large, the BMpThy chimeras recreated the picture seen in WT mice with high scores for necrosis and cellularity (Figure 5.5A & B). However, the BM chimeras had mild neutrophil infiltration, little to no cartilage necrosis and rare epidermal necrosis. It was striking to see that replacement of dermal $\gamma\delta$ T cells in BMpThy mice recapitulated results obtained with the WT mice and similarly, that BM mice mirrored $\gamma\delta$ T cell null mice (Figure 5.5C). Thus, the loss of the dermal CD103⁺ $\gamma\delta$ T cell population appears sufficient to reduce ear inflammation and damage.

Discussion

$\gamma\delta$ T cells have been proposed to play a variety of roles in the immune response to infection in mice and primates. Studies have largely relied on systemic models of infection and generally observed an increase in the number of $\gamma\delta$ T cells in the circulation. A few studies have analyzed $\gamma\delta$ T cells in the lung (73, 83), intestine (84) and genital mucosa (85) where local accumulation of $\gamma\delta$ T cells occurs. However, many

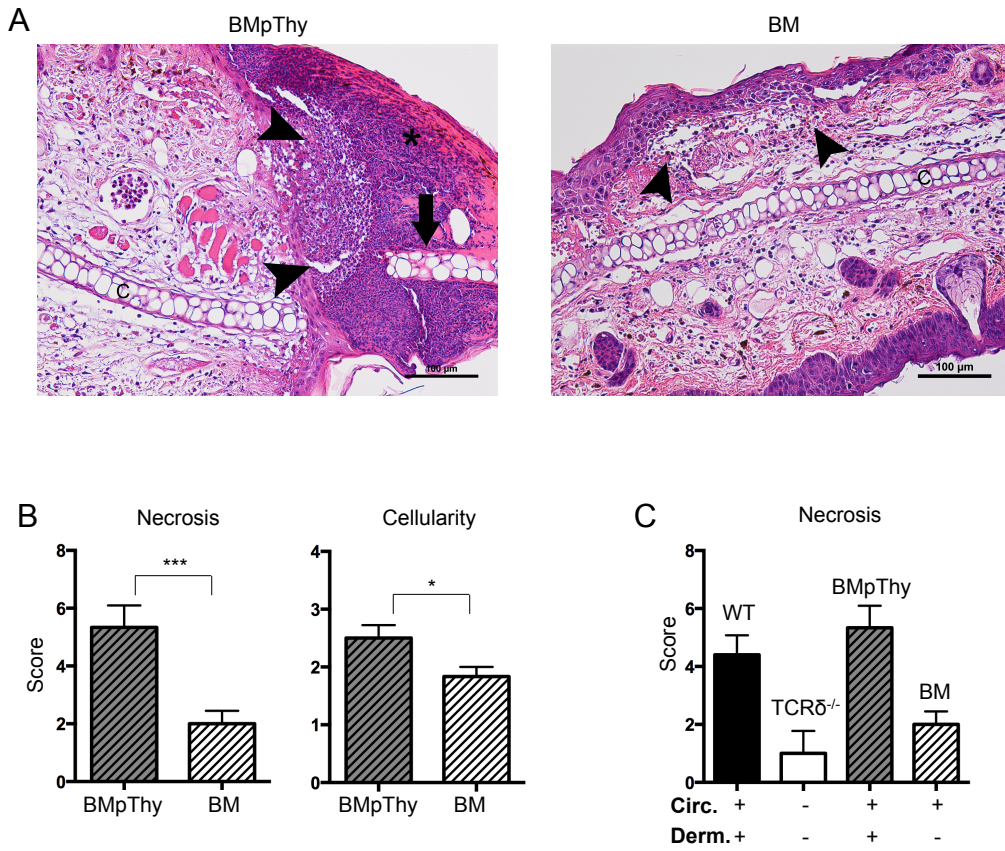


Figure 5.5. Dermal $\gamma\delta$ T cells accelerate early collateral damage and contribute to increased tissue cellularity during VV infection. Mice were infected with VV on the ear. A) Representative histological sections and B) scores for BM chimeras and BMpThy chimeras 3dpi. Mean \pm SEM is shown. C) Comparison of necrosis scores for WT, TCR $\delta^{-/-}$, BMpThy chimeras and BM chimeras in relation to the presence (+) or absence (-) of $\gamma\delta$ T cell populations (Circ = circulating $\gamma\delta$ T cells, Derm = dermal $\gamma\delta$ T cells). Arrows indicate necrotic cartilage, arrowheads indicate neutrophilic infiltrates and asterisks indicate serocellular crusts. Statistics performed with the two-tailed, unpaired student *t*-test, *n*=5-6 mice per group. **p*<0.05, ***p*<0.01, ****p*<0.005 Data are representative of >2 independent experiments, *n*=5-6 mice per group.

of these studies use systems that favor $\gamma\delta$ T cells to some extent, which inaccurately portrays their role in the immune system.

For infectious models it is often the primary goal to show increased morbidity or mortality in the mice, which lack a certain cell type or effector molecule. This has unfortunately led to studies using extremely high doses of the pathogen in order to see differences in TCR $\delta^{-/-}$ mice compared to WT (61, 65, 86). In addition to the fact that we did not see a difference in viral load with VV, our attempts to repeat previously published data in other models was not successful. Indeed we did not observe significant differences in infectious load or mortality in models of West Nile Virus or *Yersinia pseudotuberculosis* (data not shown). In addition, we also found no significant difference in the antigen specific CD8 $^{+}$ T cell response between WT and TCR $\delta^{-/-}$ mice following VV scarification or in other models of *Listeria monocytogenes* and Vesicular Stomatitis Virus infection (data not shown). Further, other experiments not included here determined that antigen presentation was not hindered in mice lacking $\gamma\delta$ T cells.

Characterization of the different $\gamma\delta$ T cell populations in the inflamed dermis confirmed the IL-17-producing capacity of CD103 $^{+}$ dermal $\gamma\delta$ T cells, even in naïve tissue. A small population of the CD103 $^{-}$ $\gamma\delta$ T cells also appeared to be capable of producing IL-17 and this was determined to be from CD27 $^{-}$ immigrants, which we predict originated from the circulating CD27 $^{-}$ CCR6 $^{-}$ population. Interestingly Granzyme B was only produced by the inflammatory recruited $\gamma\delta$ T cells and not until the peak of the response.

It was surprising however that IFN γ was not expressed at any point by $\gamma\delta$ T cells in the dermis. This was not due to technical difficulties in staining for IFN γ as we were

able to see a positive population among the $\alpha\beta$ T cells. This suggests that perhaps a subset within the CD27⁺ $\gamma\delta$ T cell population that does not possess IFN γ -producing capabilities is specifically recruited to the tissue. Alternatively they lose that ability in response to inflammatory signals upon entering the tissue. In either case, by the parameters assessed here, a large portion of the inflammatory recruited $\gamma\delta$ T cells have an unknown function the remains to be determined.

Since $\gamma\delta$ T cells appeared to be a dynamic population capable of acquiring functions in response to infection, but their loss did not impact the cytotoxic T cell response or viral titers, we took a different approach to assess what purpose they could have. Histologic analysis offered qualitative and quantitative data at the site of infection that revealed an overall more quiet state in mice that lacked all $\gamma\delta$ T cells. More specifically, it turned out to be the dermal $\gamma\delta$ T cell population that was primarily responsible for the increased cellularity and necrosis. Other studies have shown that $\gamma\delta$ T cell production of IL-17 early on contributes to neutrophil-mediated tissue damage (87) as well as enhanced inflammation (88), indicating they are active participants in the inflammatory response even if they do not play a central role. These experiments reveal that the inflammatory immigrant $\gamma\delta$ T cells have functional attributes distinct from the inflammatory resident dermal $\gamma\delta$ T cells, the latter being primarily responsible for enhancing the inflammatory response in the tissue.

Chapter 6:

Concluding remarks and future directions

Scarification of the skin with VV was used as a vaccine to eradicate small pox infection and the virus is now appreciated as an important vector for vaccine development and potentially cancer treatment (70). We have employed VV scarification of mouse ears to interrogate the distinct roles of recruited and resident dermal $\gamma\delta$ T cells and to better understand their diversity. In this study, we describe for the first time the expansion, recruitment and contraction of $\gamma\delta$ T cells in the dermis following localized VV infection. About half of the expanded dermal $\gamma\delta$ T cells at day 7 were comprised of a unique population of CD103⁻CCR6⁻ $\gamma\delta$ T cells that rapidly appeared in the dermis in response to infection (Figure 6.1). This novel population was derived primarily from circulating CD27⁺ $\gamma\delta$ T cells. A portion of the immigrant $\gamma\delta$ T cells were phenotypically similar to the CD103⁺ IL-17 producing dermal-resident $\gamma\delta$ T cell population and derived from circulating CD27⁻ $\gamma\delta$ T cells, although some were also found in the CD103⁻ fraction. These immigrant populations were functionally distinct and played a discrete role from the resident dermal population, which was ultimately responsible for driving increased cellularity and tissue damage at an early time-point.

The number of dermal $\gamma\delta$ T cells increased approximately 10-fold following VV infection and our data suggests that most of this increase can be ascribed to recruitment and immigration rather than expansion of the resident population. Thus 7×10^5 adoptively transferred $\gamma\delta$ T cells made up 5% of the total $\gamma\delta$ T cell population in the spleen and LNs before infection and this donor:host $\gamma\delta$ T cells ratio was maintained

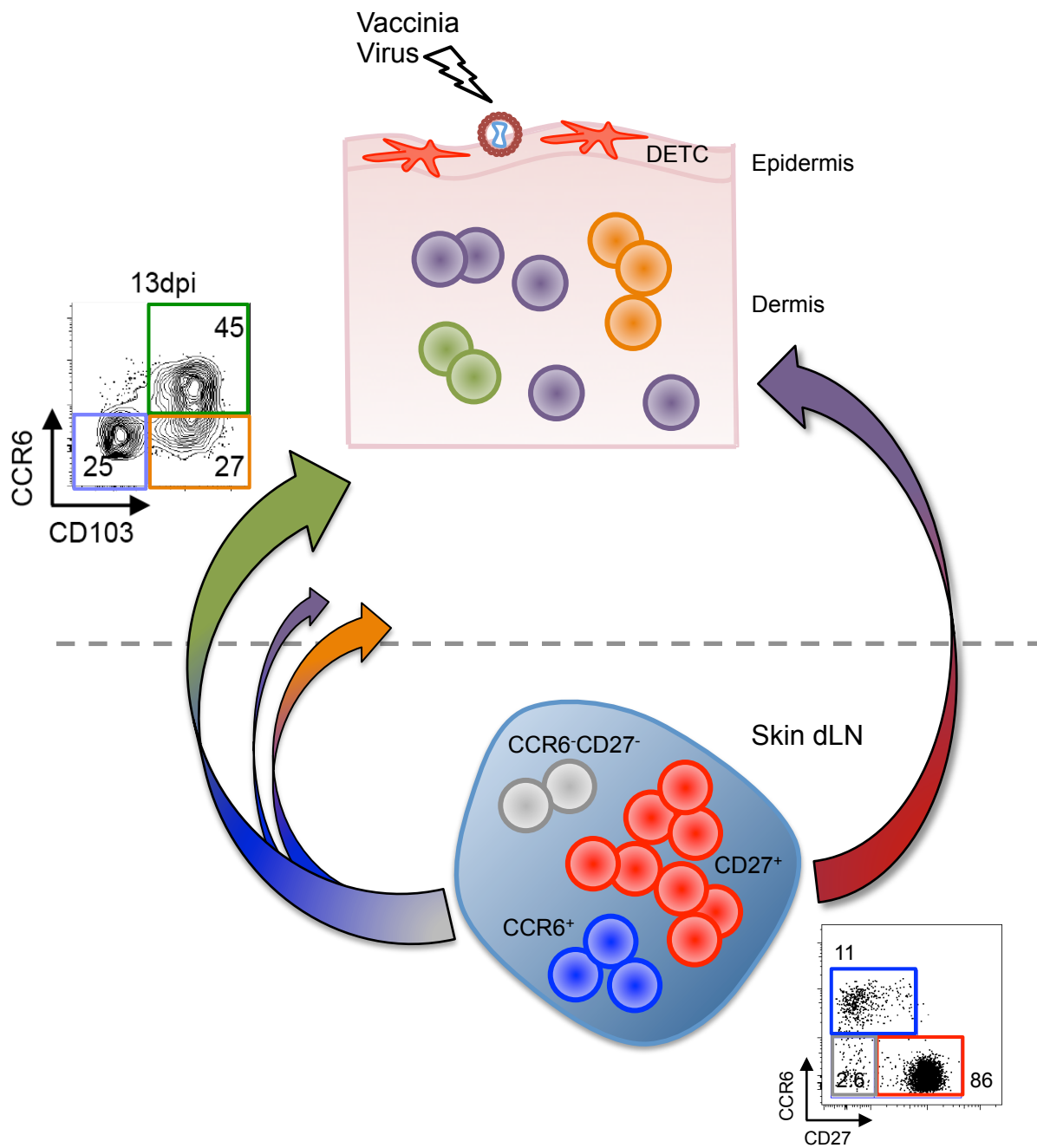


Figure 6.1. Model of $\gamma\delta$ T cell response following scarification with VV.

in the dermis at day 7 following infection. Furthermore, the CD103/CCR6 profile of the adoptively transferred immigrants resembled that of the host $\gamma\delta$ T cells in the dermis day 7 post-infection. The ability of immigrant cells to diversify into all the dermal subsets lead us to ask what the contribution was of the individual populations in the circulation. Emerging evidence confirms that CD27 delineates functional $\gamma\delta$ T cell subsets in both mice (27, 41, 43) and humans (45-47). Transfer of CD27⁺ and CD27⁻ circulating $\gamma\delta$ T cells into separate hosts followed by VV scarification demonstrated their unique contribution to CD103⁻ or CD103⁺ dermal populations, respectively. These experiments also confirmed the independent maintenance of these two populations even in the presence of inflammation. The stability of these two subsets and the constancy of the CCR6⁺ and CCR6⁻ ratio within the CD27⁻ population offer an important tool for studying $\gamma\delta$ T cells during inflammation. Although other groups have compared CD27⁺ and CCR6⁺ $\gamma\delta$ T cells (27, 41), the circulating CCR6⁻CD27⁻ subset has received less attention. This latter population is uniformly ROR γ t⁺ and distinguished from the CCR6⁺ population by lower levels of CD103 and CD44. Future studies will be needed to explore the nuances between these populations.

Although there is some disagreement concerning the radiosensitivity of $\gamma\delta$ T cells and their reconstitution in an irradiated adult mouse (27, 28, 34), our chimera experiments revealed that, unlike the DETC population, $\gamma\delta$ T cells in the circulation and dermis are radiosensitive. Our results confirm that transfer of perinatal thymocytes into an irradiated host generates bonafide CCR6⁺CD27⁻ $\gamma\delta$ T cells in the circulation and residents in the dermis. Differential kinetics and functional profiles of the BM (immigrant) and pThy (resident) $\gamma\delta$ T cell populations in the BMpThy chimeras allowed us to ask

whether they had distinct roles following infection. Determining the role of dermal $\gamma\delta$ T cells by comparing WT and TCR $\delta^{-/-}$ mice is complicated by the absence of normal DETC in the null mice (11), cells that are known to play a role in keratinocyte growth and survival, perhaps impacting tissue damage or recovery. Whole body irradiation allowed us to specifically deplete the resident dermal $\gamma\delta$ T cells, creating mice that lack this population while retaining healthy BM-derived circulating $\gamma\delta$ T cell populations. Comparing mice specifically with or without dermal $\gamma\delta$ T cells revealed that the dermal resident population was responsible for the increased inflammation observed in infected WT animals.

The ability of pThy-derived dermal $\gamma\delta$ T cells to recruit inflammatory cells, such as neutrophils, is likely due to their production of IL-17 (28, 32, 89) and recruitment of neutrophils by $\gamma\delta$ T cells directly results in increased tissue damage (87). We demonstrated increased necrosis and cellularity of infected ears 3 days after VV infection, indicating that the resident IL-17⁺ $\gamma\delta$ T cells are early responders to viral infection. In contrast, the immigrating population of CD103⁺CCR6⁻ DN $\gamma\delta$ T cells, which appeared concurrently, only upregulated Granzyme B expression at a later time-point. Although classically associated with cytotoxicity, which has been shown for $\gamma\delta$ T cells (54), Granzyme B has direct antiviral effects within cells and can cleave structural proteins when released into the extracellular matrix (90). Importantly for our study, extracellular Granzyme B release has been shown to have remodeling activity (91), potentially facilitating migration of cells into the tissue and impacting wound repair. Considering the absence of $\gamma\delta$ T cells had no effect on viral load and the number of $\gamma\delta$ T cells within the dermis remained elevated for an extended period of time, these

Granzyme-producing cells may play a non-traditional role during inflammation and in the recovery process after viral clearance. There were also large populations within both subsets that were negative for the parameters we tested. Future studies should take an unbiased approach to determine what other functions they may be performing.

Little is known about whether $\gamma\delta$ T cells can form 'memory'. The majority of studies have examined at total $\gamma\delta$ T cell population re-expansion (53, 92) or relied on CD44 expression (47), which is now appreciated to be regulated differently in $\gamma\delta$ T cells than classical $\alpha\beta$ T cells (1). When we transferred congenically marked $\gamma\delta$ T cells, none of the immigrant $\gamma\delta$ T cells remained in the dermis as residents after infection was cleared (Figure 4.1). This was true for the CD27⁺ circulating $\gamma\delta$ T cells characterized as CD103⁻CCR6⁻ DN cells in the dermis and for the CD27⁻ circulating cells that give rise to all three populations in the dermis at day 7 post infection. Similarly in the BMpThy chimeras, BM-derived circulating $\gamma\delta$ T cells that entered during the infection did not remain there long term. This indicates that inflammation is not sufficient to drive the long-term skin residence of $\gamma\delta$ T cells that enter the skin from the circulation. In contrast, it has been observed after oral *Listeria monocytogenes* infection that a population of $\gamma\delta$ T cells with memory-like function develop and persist in intestinal tissues (84). However, generating resident dermal $\gamma\delta$ T cells requires a neonatal population (or their precursors), derived in our case from the transfer of perinatal thymocytes into irradiated hosts.

The presence of pThy-derived $\gamma\delta$ T cells in the dermis was required to increase cellularity near the site of infection and to amplify the overall potency of the immune response as demonstrated by increased tissue damage in WT and BMpThy mice. While

the complete absence of $\gamma\delta$ T cells did not translate to increased viral load in this or related systems (85, 93), other models have shown that mice lacking $\gamma\delta$ T cells are more susceptible to bacterial infection (71) and have a decreased capacity for wound healing (10).

Together, the data indicate that $\gamma\delta$ T cells are a dynamic population with a range of functions, but that they might not respond equally to all inflammatory cues. Importantly, since there is no DETC counterpart in human skin (94), it has become increasingly important to isolate the relevance of $\gamma\delta$ T cells in the dermis in models relevant to human disease. Our study employing the adoptive transfer of circulating $\gamma\delta$ T cells into normal hosts and the creation of chimeras specifically lacking a dermal resident population will be useful for interrogating $\gamma\delta$ T cell subsets and furthering our understanding of the dermal immune network.

This study also challenges the notion that terminology used to describe classical $\alpha\beta$ T cells can be transferred to also characterize $\gamma\delta$ T cells. While labels such as “naïve”, “central memory” and “effector memory” have distinct meaning and are tightly correlated with cell surface proteins that are well defined for $\alpha\beta$ T cells, these same surface proteins may not carry the same meaning on $\gamma\delta$ T cells. Here we have demonstrated that CD27 stably marks separate $\gamma\delta$ T cell lineages where expression of this same protein is constitutively expressed on all naive $\alpha\beta$ T cells and can be modified by external cues (95).

Therefore, the function of a cell surface protein should be detached from its classical terminology when describing $\gamma\delta$ T cells as the purpose of their expression continues to be investigated. The expression of a marker such as CD44 on the cell

surface serves a specific function and the fact that has long been used to designate memory T cells should not influence discussion of its expression on other cell types. On $\gamma\delta$ T cells it is now appreciated that even the TCR itself may even serve a different function on the CD27⁻ population, which express high levels of CD44 – after receiving a strong TCR signal in the thymus these $\gamma\delta$ T cells are licensed to respond quickly in the periphery. Therefore CD44 expression indicates their ability to rapidly perform effector functions, perhaps similar to $\alpha\beta$ T cells, but otherwise shares no resemblance to a traditional memory response.

The fact that $\gamma\delta$ T cells have persisted over time and across species (6, 96), dominating the T cell compartment in some cases, suggests their ability to perform important functions. It is likely that many of these are redundant in organisms that have developed a dominant $\alpha\beta$ T cell population. However, this does not necessarily make $\gamma\delta$ T cell existence inconsequential in these systems. Although in many situations $\gamma\delta$ T cells may be dispensable for clearance of a pathogen, their tendency towards enhancement of immune pathology offers a clue into their usefulness in immune therapy. In settings of autoimmunity (97) or cancer (98), targeted approaches against $\gamma\delta$ T cells may prove important for modulating the immune response.

References

1. Wencker, M., G. Turchinovich, R. Di Marco Barros, L. Deban, A. Jandke, A. Cope, and A. C. Hayday. 2013. Innate-like T cells straddle innate and adaptive immunity by altering antigen-receptor responsiveness. *Nat. Immunol.* 15: 80–87.
2. Shibata, K., H. Yamada, M. Nakamura, S. Hatano, Y. Katsuragi, R. Kominami, and Y. Yoshikai. 2014. IFN- γ -producing and IL-17-producing $\gamma\delta$ T cells differentiate at distinct developmental stages in murine fetal thymus. *J. Immunol.* 192: 2210–2218.
3. Chien, Y.-H., C. Meyer, and M. Bonneville. 2013. $\gamma\delta$ T Cells: First Line of Defense and Beyond. *Annual Reviews of Immunology* 32: 121–155.
4. Xiong, N., and D. H. Raulet. 2007. Development and selection of $\gamma\delta$ T cells. *Immunol. Rev.* 215: 15–31.
5. Allison, J. P., and W. L. Havran. 1991. The immunobiology of T cells with invariant $\gamma\delta$ antigen receptors. *Annu. Rev. Immunol.* 9: 679–705.
6. Shekhar, S., S. Milling, and X. Yang. 2012. Migration of $\gamma\delta$ T cells in steady-state conditions. *Vet. Immunol. Immunop.* 147: 1–5.
7. Jin, Y., M. Xia, A. Sun, C. M. Saylor, and N. Xiong. 2010. CCR10 Is Important for the Development of Skin-Specific $\gamma\delta$ T Cells by Regulating Their Migration and Location. *J. Immunol.* 185: 5723–5731.
8. Chennupati, V., T. Worbs, X. Liu, F. H. Malinarich, S. Schmitz, J. D. Haas, B. Malissen, R. Förster, and I. Prinz. 2010. Intra- and intercompartmental movement of $\gamma\delta$ T cells: intestinal intraepithelial and peripheral $\gamma\delta$ T cells represent exclusive nonoverlapping populations with distinct migration characteristics. *J. Immunol.* 185: 5160–5168.
9. Jiang, X., J. J. Campbell, and T. S. Kupper. 2010. Embryonic trafficking of $\gamma\delta$ T cells to skin is dependent on E/P selectin ligands and CCR4. *Proc. Natl. Acad. Sci. U.S.A.* 107: 7443–7448.
10. Havran, W. L., and J. M. Jameson. 2010. Epidermal T cells and wound healing. *J. Immunol.* 184: 5423–5428.
11. Jameson, J. M., G. Cauvi, D. A. Witherden, and W. L. Havran. 2004. A keratinocyte-responsive $\gamma\delta$ TCR is necessary for dendritic epidermal T cell activation by damaged keratinocytes and maintenance in the epidermis. *J. Immunol.* 172: 3573–3579.
12. Macleod, A. S., and W. L. Havran. 2011. Functions of skin-resident $\gamma\delta$ T cells. *Cell. Mol. Life. Sci.* 68: 2399–2408.

13. Chodaczek, G., V. Papanna, M. A. Zal, and T. Zal. 2012. Body-barrier surveillance by epidermal $\gamma\delta$ TCRs. *Nat. Immunol.* 13: 272-283.
14. Komori, H. K., D. A. Witherden, R. Kelly, K. Sendaydiego, J. M. Jameson, L. Teyton, and W. L. Havran. 2012. Cutting Edge: Dendritic Epidermal $\gamma\delta$ T Cell Ligands Are Rapidly and Locally Expressed by Keratinocytes following Cutaneous Wounding. *J. Immunol.* 188: 2972–2976.
15. Hao, J., X. Wu, S. Xia, Z. Li, T. Wen, N. Zhao, Z. Wu, P. Wang, L. Zhao, and Z. Yin. 2010. Current progress in $\gamma\delta$ T-cell biology. *Cell. Mol. Immunol.* 7: 409–413.
16. Wesch, D., C. Peters, H.-H. Oberg, K. Pietschmann, and D. Kabelitz. 2011. Modulation of $\gamma\delta$ T cell responses by TLR ligands. *Cell. Mol. Life. Sci.* 68: 2357–2370.
17. Tong, P. L., B. Roediger, N. Kolesnikoff, M. Biro, S. S. Tay, R. Jain, L. E. Shaw, M. A. Grimbaldston, and W. Weninger. 2014. The Skin Immune Atlas: Three-dimensional analysis of cutaneous leukocyte subsets by multiphoton microscopy. *J. Invest. Dermatol.* doi:10.1038/jid.2014.289.
18. Heath, W. R., and F. R. Carbone. 2013. The skin-resident and migratory immune system in steady state and memory: innate lymphocytes, dendritic cells and T cells. *Nat. Immunol.* 14: 978–985.
19. Zaid, A., L. K. Mackay, A. Rahimpour, A. Braun, M. Veldhoen, F. R. Carbone, J. H. Manton, W. R. Heath, and S. N. Mueller. 2014. Persistence of skin-resident memory T cells within an epidermal niche. *Proc. Natl. Acad. Sci. U.S.A.* 111: 5307–5312.
20. Wakim, L. M., N. Gupta, J. D. Mintern, and J. A. Villadangos. 2013. Enhanced survival of lung tissue-resident memory CD8⁺ T cells during infection with influenza virus due to selective expression of IFITM3. *Nat. Immunol.* 3: 238–245.
21. Wakim, L. M., A. Woodward-Davis, and M. J. Bevan. 2010. Memory T cells persisting within the brain after local infection show functional adaptations to their tissue of residence. *Proc. Natl. Acad. Sci. U.S.A.* 107: 17872–17879.
22. Gebhardt, T., L. M. Wakim, L. Eidsmo, P. C. Reading, W. R. Heath, and F. R. Carbone. 2009. Memory T cells in nonlymphoid tissue that provide enhanced local immunity during infection with herpes simplex virus. *Nat. Immunol.* 10: 524–530.
23. Mackay, L. K., A. T. Stock, J. Z. Ma, C. M. Jones, S. J. Kent, S. N. Mueller, W. R. Heath, F. R. Carbone, and T. Gebhardt. 2012. Long-lived epithelial immunity by tissue-resident memory T (TRM) cells in the absence of persisting local antigen presentation. *Proc. Natl. Acad. Sci. U.S.A.* 109: 7037–7042.

24. Jiang, X., R. A. Clark, L. Liu, A. J. Wagers, R. C. Fuhlbrigge, and T. S. Kupper. 2012. Skin infection generates non-migratory memory CD8⁺ TRM cells providing global skin immunity. *Nature* 483: 227–231.
25. Shibata, K. 2012. Close link between development and function of $\gamma\delta$ T cells. *Microbiol. Immunol.* 56: 217–227.
26. Bandeira, A., T. Mota-Santos, S. Itohara, S. Degermann, C. Heusser, S. Tonegawa, and A. Coutinho. 1990. Localization of $\gamma\delta$ T cells to the intestinal epithelium is independent of normal microbial colonization. *J. Exp. Med.* 172: 239–244.
27. Haas, J. D., S. Ravens, S. Düber, I. Sandrock, L. Oberdörfer, E. Kashani, V. Chennupati, L. Föhse, R. Naumann, S. Weiss, A. Krueger, R. Förster, and I. Prinz. 2012. Development of Interleukin-17-producing $\gamma\delta$ T cells is restricted to a functional embryonic wave. *Immunity* 37: 48–59.
28. Sumaria, N., B. Roediger, L. G. Ng, J. Qin, R. Pinto, L. L. Cavanagh, E. Shklovskaya, B. Fazekas de St Groth, J. A. Triccas, and W. Weninger. 2011. Cutaneous immunosurveillance by self-renewing dermal $\gamma\delta$ T cells. *J. Exp. Med.* 208: 505–518.
29. Holtmeier, W., M. Pfander, A. Hennemann, T. M. Zollner, R. Kaufmann, and W. F. Caspary. 2001. The TCR δ repertoire in normal human skin is restricted and distinct from the TCR δ repertoire in the peripheral blood. *J. Invest. Dermatol.* 116: 275–280.
30. Maher, B. M., M. E. Mulcahy, A. G. Murphy, M. Wilk, K. M. O'Keeffe, J. A. Geoghegan, E. C. Lavelle, and R. M. McLoughlin. 2013. Nlrp-3-driven Interleukin 17 production by $\gamma\delta$ T cells controls infection outcomes during *Staphylococcus aureus* surgical site infection. *Infect. Immun.* 81: 4478–4489.
31. Byamba, D., D. Y. Kim, D.-S. Kim, T.-G. Kim, H. Jee, S. H. Kim, T.-Y. Park, S.-H. Yang, S.-K. Lee, and M.-G. Lee. 2014. Skin-penetrating methotrexate alleviates imiquimod-induced psoriasiform dermatitis via decreasing IL-17-producing $\gamma\delta$ T cells. *Exp. Dermatol.* 23: 492–496.
32. Gray, E. E., F. Ramírez-Valle, Y. Xu, S. Wu, Z. Wu, K. E. Karjalainen, and J. G. Cyster. 2013. Deficiency in IL-17-committed V γ 4⁺ $\gamma\delta$ T cells in a spontaneous Sox13-mutant CD45.1⁺ congenic mouse substrain provides protection from dermatitis. *Nat. Immunol.* 14: 584–592.
33. Cai, Y., X. Shen, C. Ding, C. Qi, K. Li, X. Li, V. R. Jala, H.-G. Zhang, T. Wang, J. Zheng, and J. Yan. 2011. Pivotal role of dermal IL-17-producing $\gamma\delta$ T cells in skin inflammation. *Immunity* 35: 596–610.

34. Gray, E. E., K. Suzuki, and J. G. Cyster. 2011. Cutting Edge: Identification of a motile IL-17-producing $\gamma\delta$ T cell population in the dermis. *J. Immunol.* 186: 6091–6095.
35. Haas, J. D., F. H. M. Gonzalez, S. Schmitz, V. Chennupati, L. Föhse, E. Kremmer, R. Förster, and I. Prinz. 2009. CCR6 and NK1.1 distinguish between IL-17A and IFN γ producing $\gamma\delta$ effector T cells. *Eur. J. Immunol.* 39: 3488–3497.
36. Zhu, J., F. Hladik, A. Woodward, A. Klock, T. Peng, C. Johnston, M. Remington, A. Magaret, D. M. Koelle, A. Wald, and L. Corey. 2009. Persistence of HIV-1 receptor-positive cells after HSV-2 reactivation is a potential mechanism for increased HIV-1 acquisition. *Nat. Med.* 15: 886–892.
37. Prinz, I., A. Sansoni, A. Kissenpfennig, L. Ardouin, M. Malissen, and B. Malissen. 2006. Visualization of the earliest steps of $\gamma\delta$ T cell development in the adult thymus. *Nat. Immunol.* 7: 995–1003.
38. Heilig, J. S., and S. Tonegawa. 1986. Diversity of murine γ genes and expression in fetal and adult T lymphocytes. *Nat. Immunol.* 322: 836–840.
39. Itohara, S., P. Mombaerts, J. Lafaille, J. Iacomini, A. Nelson, A. R. Clarke, M. L. Hooper, A. Farr, and S. Tonegawa. 1993. T cell receptor δ gene mutant mice: independent generation of $\alpha\beta$ T cells and programmed rearrangements of $\gamma\delta$ TCR genes. *Cell* 72: 337–348.
40. Ribot, J. C., M. Chaves-Ferreira, F. d'Orey, M. Wencker, N. Gonçalves-Sousa, J. Decalf, J. P. Simas, A. C. Hayday, and B. Silva-Santos. 2010. Cutting edge: adaptive versus innate receptor signals selectively control the pool sizes of murine IFN- γ - or IL-17-producing $\gamma\delta$ T cells upon infection. *J. Immunol.* 185: 6421–6425.
41. Schmolka, N., K. Serre, A. R. Grosso, M. Rei, D. J. Pennington, A. Q. Gomes, and B. Silva-Santos. 2013. Epigenetic and transcriptional signatures of stable versus plastic differentiation of proinflammatory $\gamma\delta$ T cell subsets. *Nat. Immunol.* 14: 1093–1100.
42. Jensen, K. D. C., X. Su, S. Shin, L. Li, S. Youssef, S. Yamasaki, L. Steinman, T. Saito, R. M. Locksley, M. M. Davis, N. Baumgarth, and Y.-H. Chien. 2008. Thymic selection determines $\gamma\delta$ T cell effector fate: antigen-naïve cells make Interleukin-17 and antigen-experienced cells make Interferon γ . *Immunity* 29: 90–100.
43. Ribot, J. C., A. deBarros, D. J. Pang, J. F. Neves, V. Peperzak, S. J. Roberts, M. Girardi, J. Borst, A. C. Hayday, D. J. Pennington, and B. Silva-Santos. 2009. CD27 is a thymic determinant of the balance between interferon- γ - and interleukin 17-producing $\gamma\delta$ T cell subsets. *Nat. Immunol.* 10: 427–436.
44. Born, W. K., and R. L. O'Brien. 2011. $\gamma\delta$ T cells develop, respond and survive – with a little help from CD27. *Eur. J. Immunol.* 41: 26–28.

45. deBarros, A., M. Chaves-Ferreira, F. d'Orey, J. C. Ribot, and B. Silva-Santos. 2010. CD70-CD27 interactions provide survival and proliferative signals that regulate T cell receptor-driven activation of human $\gamma\delta$ peripheral blood lymphocytes. *Eur. J. Immunol.* 41: 195–201.
46. Caccamo, N., C. La Mendola, V. Orlando, S. Meraviglia, M. Todaro, G. Stassi, G. Sireci, J. J. Fournie, and F. Dieli. 2011. Differentiation, phenotype, and function of interleukin-17-producing human V γ 9V δ 2 T cells. *Blood* 118: 129–138.
47. Dieli, F., F. Poccia, M. Lipp, G. Sireci, N. Caccamo, C. Di Sano, and A. Salerno. 2003. Differentiation of effector/memory V δ 2 T cells and migratory routes in lymph nodes or inflammatory sites. *J. Exp. Med.* 198: 391–397.
48. Prinz, I. 2011. Dynamics of the interaction of $\gamma\delta$ T cells with their neighbors in vivo. *Cell. Mol. Life. Sci.* 68: 2391–2398.
49. Stewart, C. A., T. Walzer, S. H. Robbins, B. Malissen, E. Vivier, and I. Prinz. 2007. Germ-line and rearranged Tcr δ transcription distinguish bona fide NK cells and NK-like $\gamma\delta$ T cells. *Eur. J. Immunol.* 37: 1442–1452.
50. Havran, W. L. 2000. A role for epithelial $\gamma\delta$ T cells in tissue repair. *Immunol. Res.* 21: 63–69.
51. Wang, L., A. Kamath, H. Das, L. Li, and J. F. Bukowski. 2001. Antibacterial effect of human V γ 2V δ 2 T cells in vivo. *J. Clin. Invest.* 108: 1349–1357.
52. Wiemer, D. F., and A. J. Wiemer. 2014. Opportunities and challenges in development of phosphoantigens as V γ 9V δ 2 T cell agonists. *Biochem. Pharmacol.* 89: 301–312.
53. Shao, L., D. Huang, H. Wei, R. C. Wang, C. Y. Chen, L. Shen, W. Zhang, J. Jin, and Z. W. Chen. 2009. Expansion, reexpansion, and recall-like expansion of V γ 2V δ 2 T cells in smallpox vaccination and monkeypox virus infection. *J. Virol.* 83: 11959–11965.
54. Qin, G., H. Mao, J. Zheng, S. F. Sia, Y. Liu, P. L. Chan, K.-T. Lam, J. S. M. Peiris, Y.-L. Lau, and W. Tu. 2009. Phosphoantigen-expanded human $\gamma\delta$ T cells display potent cytotoxicity against monocyte-derived macrophages infected with human and avian Influenza viruses. *J. Immunol.* 200: 858–865.
55. Viey, E., C. Lucas, F. Romagne, B. Escudier, S. Chouaib, and A. Caignard. 2008. Chemokine receptors expression and migration potential of tumor-infiltrating and peripheral-expanded V γ 9V δ 2 T cells from renal cell carcinoma patients. *J. Immunother.* 31: 313–323.
56. Das, H., L. Wang, A. Kamath, and J. F. Bukowski. V γ 2V δ 2 T-cell receptor-mediated recognition of aminobisphosphonates. *Blood* 98: 1616–1618.

57. Girardi, M., D. E. Oppenheim, C. R. Steele, J. M. Lewis, E. Glusac, R. Filler, P. Hobby, B. Sutton, R. E. Tigelaar, and A. C. Hayday. 2001. Regulation of cutaneous malignancy by $\gamma\delta$ T cells. *Science* 294: 605–609.
58. Kong, Y., W. Cao, X. Xi, C. Ma, L. Cui, and W. He. 2009. The NKG2D ligand ULBP4 binds to TCR 9/ 2 and induces cytotoxicity to tumor cells through both TCR $\gamma\delta$ and NKG2D. *Blood* 114: 310–317.
59. Paul, S., A. K. Singh, Shilpi, and G. Lal. 2013. Phenotypic and functional plasticity of damma–delta ($\gamma\delta$) T cells in inflammation and tolerance. *Int. Rev. Immunol.* 33: 537–538.
60. Maloy, K. J., B. Odermatt, H. Hengartner, and R. M. Zinkernagel. 1998. Interferon γ -producing $\gamma\delta$ T cell-dependent antibody isotype switching in the absence of germinal center formation during virus infection. *Proc. Natl. Acad. Sci. U.S.A.* 95: 1160–1165.
61. Selin, L. K., P. A. Santolucito, A. K. Pinto, E. Szomolanyi-Tsuda, and R. M. Welsh. 2001. Innate immunity to viruses: control of vaccinia virus infection by $\gamma\delta$ T cells. *J. Immunol.* 166: 6784–6794.
62. Mann, E. R., N. E. McCarthy, S. T. C. Peake, A. N. Milestone, H. O. Al-Hassi, D. Bernardo, C. T. Tee, J. Landy, M. C. Pitcher, S. A. Cochrane, A. L. Hart, A. J. Stagg, and S. C. Knight. 2012. Skin- and gut-homing molecules on human circulating $\gamma\delta$ T cells and their dysregulation in inflammatory bowel disease. *J. Trans. Immunol.* 170: 122–130.
63. Argentati, K., F. Re, S. Serresi, M. G. Tucci, B. Bartozzi, G. Bernardini, and M. Provinciali. 2003. Reduced number and impaired function of circulating $\gamma\delta$ T cells in patients with cutaneous primary melanoma. *J. Invest. Dermatol.* 120: 829–834.
64. Laggner, U., P. Di Meglio, G. K. Perera, C. Hundhausen, K. E. Lacy, N. Ali, C. H. Smith, A. C. Hayday, B. J. Nickoloff, and F. O. Nestle. Identification of a novel proinflammatory human skin-homing V γ 9V δ 2 T cell subset with a potential role in psoriasis. *J. Immunol.* 187: 2783–2793.
65. Wang, T., E. Scully, Z. Yin, J. H. Kim, S. Wang, J. Yan, M. Mamula, J. F. Anderson, J. Craft, and E. Fikrig. 2003. IFN- γ -producing $\gamma\delta$ T cells help control murine West Nile virus infection. *J. Immunol.* 171: 2524–2531.
66. Pennington, D. J., B. Silva-Santos, J. Shires, E. Theodoridis, C. Pollitt, E. L. Wise, R. E. Tigelaar, M. J. Owen, and A. C. Hayday. 2003. The inter-relatedness and interdependence of mouse T cell receptor $\gamma\delta$ ⁺ and $\alpha\beta$ ⁺ cells. *Nat. Immunol.* 4: 991–998.
67. Tschärke, D. C., and G. L. Smith. 1999. A model for vaccinia virus pathogenesis and immunity based on intradermal injection of mouse ear pinnae. *J. Gen. Virol.* 80: 2751–2755.

68. Scholzen, T., and J. Gerdes. 2000. The Ki-67 protein: From the known and the unknown. *J. Cell. Phys.* 182: 311–322.
69. Webber, B. J., J. R. Montgomery, A. E. Markelz, K. C. Allen, J. C. Hunninghake, S. A. Ritchie, M. T. Pawlak, L. A. Johnston, T. A. Oliver, and B. S. Winterton. 2014. Spread of Vaccinia Virus Through Shaving During Military Training. *Med. Surv. Month. Report.* 21: 1–23.
70. Veradi, P. H., A. Titong, and C. J. Hagen. 2012. A vaccinia virus renaissance: new vaccine and immunotherapeutic uses after smallpox eradication. *Hu. Vac. Immuno.* 8: 961–970.
71. Hamada, S., M. Umemura, T. Shiono, K. Tanaka, A. Yahagi, M. D. Begum, K. Oshiro, Y. Okamoto, H. Watanabe, K. Kawakami, C. Roark, W. K. Born, R. O'Brien, K. Ikuta, H. Ishikawa, S. Nakae, Y. Iwakura, T. Ohta, and G. Matsuzaki. 2008. IL-17A produced by $\gamma\delta$ T cells plays a critical role in innate immunity against *Listeria monocytogenes* infection in the liver. *J. Immunol.* 181: 3456–3463.
72. Sutton, C. E., S. J. Lalor, C. M. Sweeney, C. F. Brereton, E. C. Lavelle, and K. H. G. Mills. 2009. Interleukin-1 and IL-23 induce innate IL-17 production from $\gamma\delta$ T cells, amplifying Th17 responses and autoimmunity. *Immunity* 31: 331–341.
73. Dodd, J., S. Riffault, J. S. Kodituwakku, A. C. Hayday, and P. J. M. Openshaw. 2009. Pulmonary $V\gamma 4^+$ $\gamma\delta$ T cells have proinflammatory and antiviral effects in viral lung disease. *J. Immunol.* 182: 1174–1181.
74. Wu, Y., W. Wu, W. M. Wong, E. Ward, A. J. Thrasher, D. Goldblatt, M. Osman, P. Digard, D. H. Canaday, and K. Gustafsson. 2009. Human $\gamma\delta$ T cells: a lymphoid lineage cell capable of professional phagocytosis. *J. Immunol.* 183: 5622–5629.
75. Brandes, M., K. Willimann, G. Bioley, N. Lévy, M. Eberl, M. Luo, R. Tampé, F. Lévy, P. Romero, and B. Moser. 2009. Cross-presenting human $\gamma\delta$ T cells induce robust CD8+ $\alpha\beta$ T cell responses. *Proc. Natl. Acad. Sci. U.S.A.* 106: 2307–2312.
76. Himoudi, N., D. A. Morgenstern, M. Yan, B. Vernay, L. Saraiva, Y. Wu, C. J. Cohen, K. Gustafsson, and J. Anderson. 2012. Human $\gamma\delta$ T lymphocytes are licensed for professional antigen presentation by interaction with opsonized target cells. *J. Immunol.* 188: 1708–1716.
77. Cheng, L., Y. Cui, H. Shao, G. Han, L. Zhu, Y. Huang, R. L. O'Brien, W. K. Born, H. J. Kaplan, and D. Sun. 2008. Mouse $\gamma\delta$ T cells are capable of expressing MHC class II molecules, and of functioning as antigen-presenting cells. *J. Neuroimmunol.* 203: 3–11.
78. Brandes, M., K. Willimann, and B. Moser. 2005. Professional antigen-presentation function by human $\gamma\delta$ T Cells. *Science* 309: 264–268.

79. Meuter, S., M. Eberl, and B. Moser. 2010. Prolonged antigen survival and cytosolic export in cross-presenting human $\gamma\delta$ T cells. *Proc. Natl. Acad. Sci. U.S.A.* 107: 8730–8735.
80. Leslie, D. S., M. S. Vincent, F. M. Spada, H. Das, M. Sugita, C. T. Morita, and M. B. Brenner. 2002. CD1-mediated $\gamma\delta$ T cell maturation of dendritic cells. *J. Exp. Med.* 196: 1575–1584.
81. Wang, T., Y. Gao, E. Scully, C. T. Davis, J. F. Anderson, T. Welte, M. Ledizet, R. Koski, J. A. Madri, A. Barrett, Z. Yin, J. Craft, and E. Fikrig. 2006. $\gamma\delta$ T cells facilitate adaptive immunity against West Nile virus infection in mice. *J. Immunol.* 177: 1825–1832.
82. Kalyan, S., and D. Kabelitz. 2014. When neutrophils meet T cells: Beginnings of a tumultuous relationship with underappreciated potential. *Eur. J. Immunol.* 44: 627–633.
83. Huang, D., C. Y. Chen, Z. Ali, L. Shao, L. Shen, H. A. Lockman, R. E. Barnewall, C. Sabourin, J. Eestep, A. Reichenberg, M. Hintz, H. Jomaa, R. Wang, and Z. W. Chen. 2009. Antigen-specific V γ 2V δ 2 T effector cells confer homeostatic protection against pneumonic plaque lesions. *Proc. Natl. Acad. Sci. U.S.A.* 106: 7553–7558.
84. Sheridan, B. S., P. A. Romagnoli, Q.-M. Pham, H.-H. Fu, F. Alonzo III, W.-D. Schubert, N. E. Freitag, and L. LeFrancois. 2013. $\gamma\delta$ T cells exhibit multifunctional and protective memory in intestinal tissues. *Immunity* 39: 184–195.
85. Kim, J.-O., H.-R. Cha, E.-D. Kim, and M.-N. Kweon. 2012. Pathological effect of IL-17A-producing TCR $\gamma\delta$ ⁺ T cells in mouse genital mucosa against HSV-2 infection. *Immunol. Lett.* 147: 34–40.
86. Moretto, M., B. Durell, J. D. Schwartzman, and I. A. Khan. 2001. $\gamma\delta$ T cell-deficient mice have a down-regulated CD8⁺ T cell immune response against Encephalitozoon cuniculi infection. *J. Immunol.* 166: 7389–7397.
87. Toth, B., M. Alexander, T. Daniel, I. H. Chaudry, W. J. Hubbard, and M. G. Schwacha. 2004. The role of $\gamma\delta$ T cells in the regulation of neutrophil-mediated tissue damage after thermal injury. *J. Leukocyte. Biol.* 76: 545–552.
88. Roark, C. L., J. D. French, M. A. Taylor, A. M. Bendele, W. K. Born, and R. L. O'Brien. 2007. Exacerbation of collagen-induced arthritis by clonal, IL-17-producing $\gamma\delta$ T cells. *J. Immunol.* 179: 5576–5583.
89. Shibata, K., H. Yamada, H. Hara, K. Kishihara, and Y. Yoshikai. 2007. Resident V δ 1⁺ $\gamma\delta$ T cells control early infiltration of neutrophils after Escherichia coli infection via IL-17 production. *J. Immunol.* 178: 4466–4472.

90. Romero, V., and F. Andrade. 2008. Non-apoptotic functions of granzymes. *Tissue Antigens* 71: 409–416.
91. Buzza, M. S., L. Zamurs, J. Sun, C. H. Bird, A. I. Smith, J. A. Trapani, C. J. Froelich, E. C. Nice, and P. I. Bird. 2005. Extracellular matrix remodeling by human Granzyme B via cleavage of vitronectin, fibronectin, and laminin. *J. Biol. Chem.* 280: 23549–23558.
92. Shen, Y., D. Zhou, L. Qiu, X. Lai, M. Simon, L. Shen, Z. Kou, Q. Wang, L. Jiang, J. Estep, R. Hunt, M. Clagett, P. K. Sehgal, Y. Li, X. Zeng, C. T. Morita, M. B. Brenner, N. L. Letvin, and Z. W. Chen. 2002. Adaptive immune response of V γ 2V δ 2+ T cells during mycobacterial infections. *Science* 295: 2255–2258.
93. McCarthy, M. K., L. Zhu, M. C. Procaro, and J. B. Weinberg. 2014. IL-17 contributes to neutrophil recruitment but not to control of viral replication during acute mouse adenovirus type 1 respiratory infection. *Virology* 456-457: 259–267.
94. Elbe, A. 1996. T-Cell receptor $\alpha\beta$ and $\gamma\delta$ T cells in rat and human skin — are they equivalent? *Semin. Immunol.* 8: 341–349.
95. Croft, M. 2014. The TNF family in T cell differentiation and function – Unanswered questions and future directions. *Semin. Immunol.* 26: 183–190.
96. Hirano, M., P. Guo, N. McCurley, M. Schorpp, S. Das, T. Boehm, and M. D. Cooper. 2013. Evolutionary implications of a third lymphocyte lineage in lampreys. *Nature* 501: 435–438.
97. Mabuchi, T., T. P. Singh, T. Takekoshi, G.-F. Jia, X. Wu, M. C. Kao, I. Weiss, J. M. Farber, and S. T. Hwang. 2012. CCR6 Is required for epidermal trafficking of $\gamma\delta$ T cells in an IL-23-induced model of psoriasiform dermatitis. *J. Invest. Dermatol.* 133: 164–171.
98. Ebert, L. M., S. Meuter, and B. Moser. 2006. Homing and function of human skin $\gamma\delta$ T cells and NK cells: Relevance for tumor surveillance. *J. Immunol.* 176: 4331-4336.